ELSEVIER

Marine and Petroleum Geology 23 (2006) 213–239

Marine and Petroleum Geology

www.elsevier.com/locate/marpetgeo

Geochemical characterisation and genetic origin of oils and condensates in the South Viking Graben, Norway

H. Justwan[a,*], B. Dahl[a], G.H. Isaksen[b]

[a]*Department of Earth Science, University of Bergen, Allegaten 41, 5007 Bergen, Norway*
[b]*ExxonMobil Exploration Company, 233 Benmar, Houston, TX 77210, USA*

Received 28 December 2004; received in revised form 14 July 2005; accepted 15 July 2005

Abstract

Geochemical analysis of oil and condensate samples from all major fields and discoveries in the Norwegian South Viking Graben, as well as source rock extracts of Upper and Middle Jurassic source horizons, was carried out to characterise reservoired hydrocarbons and establish genetic relationships. The South Viking Graben is in a mature phase of exploration, and this study aims at unravelling regional trends to improve predictions in exploration and will show the significance of the play models in the area.

Seven hydrocarbon families have been identified, based on interpretation of molecular and isotopic characteristics and multivariate analysis of biomarker data. These families can be linked to three source horizons. Three families originate from different facies of the Draupne Formation and are characterised by Pr/Ph ratios below 2, dominance of C_{27} regular steranes over the C_{29} homologues, and carbon isotopic values for saturate and aromatic fraction lighter than -28 and -27‰, respectively. The Upper Jurassic Heather Formation and the Middle Jurassic Vestland Group each source one group of hydrocarbons. Typical for Heather sourced hydrocarbons are elevated Pr/Ph ratios between 2.35 and 3.08, low ratios of C_{27}/C_{29} regular steranes and average isotopic values of -28.4‰ (δ^{13}C Sat) and -26.8‰ (δ^{13}C Aro). Hydrocarbons from a Middle Jurassic source are characterised by very heavy isotopic composition, highest Pr/Ph ratios of the data set and dominance of C_{29} regular steranes over the C_{27} homologues, among other factors. The two remaining families represent mixtures from Upper and Middle Jurassic sources, and are mainly encountered in the Greater Sleipner Area.

The available data in this study allowed characterisation of 84% of the recoverable oil resources which proved that the main source rock in the area is the Upper Jurassic Draupne Formation. The play concept including a Draupne source and Tertiary reservoir proves to be most prolific, with 239×10^6 S m^3 of recoverable oil, equalling 88% of the total characterised oil resources. Oils in these Tertiary reservoirs are however likely to be affected by biodegradation. Based on the available data, the zone of biodegradation in the South Viking Graben appears to be limited to depths above 2140 m and temperatures below 70 °C.

Keywords: North Sea; South Viking Graben; Petroleum systems; Correlation; Oil; Biomarkers; Isotopes; Biodegradation

1. Introduction

The Norwegian South Viking Graben has been explored since the late 1960s. Recoverable resources from fields and discoveries account for 323×10^6 S m^3 oil and 463×10^9 S m^3 gas (Ministry of Petroleum and Energy, 2005). Although the area may be viewed as being in a 'mature' phase of exploration, discoveries are still being made, for example the 'West Cable' discovery made by Esso Norway in the Greater Utsira High area. To optimise future exploration efforts, a thorough understanding of the petroleum systems operating in the area is necessary. Integration of existing work as well as the regional analysis of source rocks, discovered hydrocarbons, migration pathways and thermal maturity modelling of the area is essential.

This is the second part of a larger study of the petroleum systems in the South Viking Graben. Previous studies (Justwan and Dahl, 2005; Justwan et al., 2005) focussed on the distribution and quality of the Jurassic source rocks and their geochemical properties. In the present study, we analysed 66 hydrocarbon samples from 31 fields and discoveries in the area to define their thermal maturity,

* Corresponding author. Tel.: +47 5558 8116; fax: +47 5558 3660.
E-mail address: holger.justwan@geo.uib.no (H. Justwan).

0264-8172/$ - see front matter © 2005 Elsevier Ltd. All rights reserved.
doi:10.1016/j.marpetgeo.2005.07.003

composition and secondary alteration and to classify the hydrocarbons into genetic families related to specific source horizons. Based on published estimates of recoverable resources in the area (Ministry of Petroleum and Energy, 2005) and the identified hydrocarbon families, we will also attempt to evaluate the prospectivity of play concepts in the area in terms of recoverable resources. The geographic distribution of the identified genetic families will also be discussed in a migrational context.

2. Geological setting

The study area is located between 60°15′ and 58°N in the southern part of the Norwegian Viking Graben (Fig. 1). The area contains several major oil and gas accumulations, among those the Sleipner, Balder, Grane, Heimdal and Frigg fields and is dominated by a large structural high, the Utsira High, with the Stord Basin to the east and the Heimdal and Gudrun Terraces and Viking Graben to the west (Fig. 1). The main boundary of the South Viking Graben to the west is the East Shetland Platform boundary fault. This structural configuration is mainly the result of two major phases of extension during the Permo-Triassic and the Late Jurassic (Ziegler, 1992).

There are four major confirmed plays in the area (Eriksen et al., 2003): The Paleogene play, the Upper Jurassic play, the Early to Middle Jurassic play and the Triassic play. Common to all fields and discoveries of the Triassic play, is the fact that the reservoir is unconformably overlain by Upper Jurassic or Cretaceous fine-grained organically enriched rocks (Pegrum and Spencer, 1990). Hydrocarbons usually have short migration routes, and typically occur in tilted fault blocks (Goldsmith et al., 2003). One example for this play is the Sigyn field (Fig. 1) with hydrocarbons trapped in the Skagerrak Formation.

The Early to Middle Jurassic play in the area comprises hydrocarbons in the non-marine to marginal marine sands of the Lower Jurassic Statfjord Formation sealed by the Dunlin shales. In addition, the Callovian sandstones of the Hugin Formation and the Bathonian to Bajocian coastal plain sandstones of the Sleipner Formation (Pegrum and Spencer, 1990) are hydrocarbon bearing in the southern section of the study area, while in the northern half of the study area hydrocarbons are encountered in the sands of the prograding clastic wedge of the Brent delta. Tilted fault blocks are unconformably overlain by Upper Jurassic or Cretaceous shales forming the traps (Pegrum and Spencer, 1990; Husmo et al., 2003), but a domal component caused by halokinesis of Permian salt is evident in the Sleipner area (Ranaweera, 1987). Source rocks in this play are the Upper and Middle Jurassic shales, carbargillites and coals (Isaksen et al., 2002).

Syn-rift submarine fans of the Brae trend (Stow et al., 1982; Fraser et al., 2003) exemplify the Upper Jurassic play including intra Draupne and Heather Formation sands as

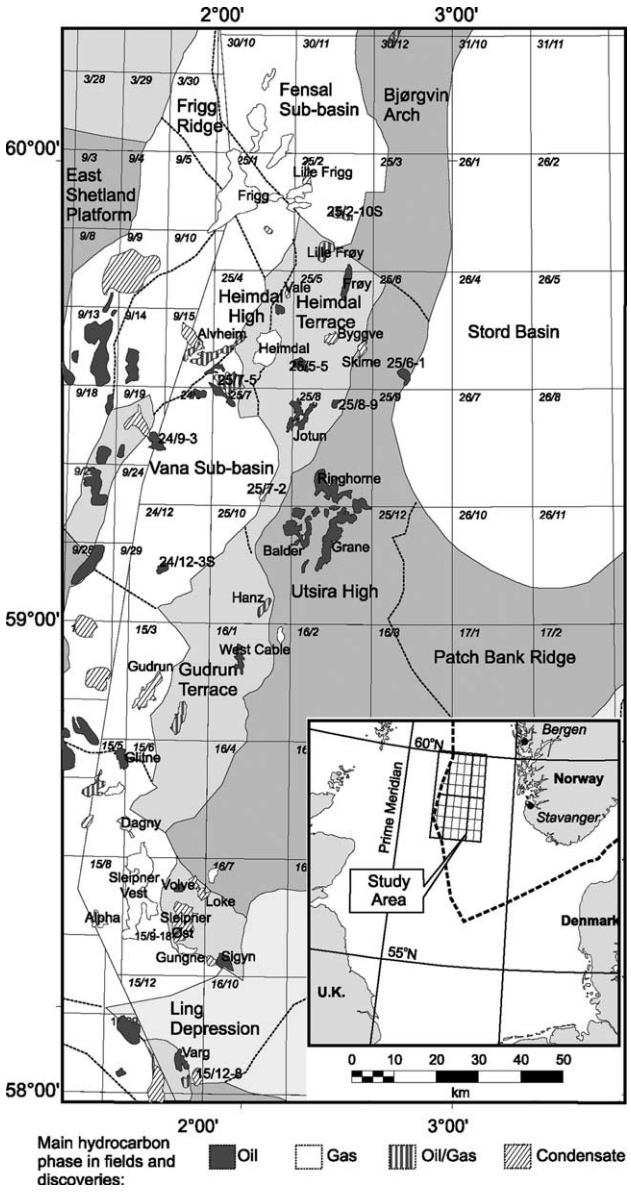

Fig. 1. Major structural elements, fields and discoveries in the study area. The study area comprises the Norwegian South Viking Graben and the adjacent Utsira High to the east.

well as the shallow marine sands deposited close to highs and basin margins (Johnson and Fisher, 1998; Fraser et al., 2003). The trapping style is variable and includes rotated fault blocks and stratigraphic traps (Pegrum and Spencer, 1990). Cap rock is most commonly the shale of the Draupne Formation. Migration is usually of short distance (Fraser et al., 2003) directly from nearby Upper Jurassic shales. Examples for this play are the Gudrun field and discovery 25/7-2 (Fig. 1).

Of great economic importance in the study area, especially in the Greater Utsira High area, is the Paleogene play, including the Paleocene (e.g. the Heimdal and Grane Fields, Fig. 1) and the Post-Paleocene plays (e.g. the Frigg Field, Fig. 1). Reservoir rocks are submarine fan sandstones

that developed along the faulted basin margins in the west and spread eastwards (Hanslien, 1987; Stewart, 1987; Milton et al., 1990; Ahmadi et al., 2003). Although the exact mechanisms of migration remain unclear (Ahmadi et al., 2003), it has been suggested that the sandstones of Paleocene, Eocene or even Oligocene age (e.g. in Well 25/2-10S) are charged by leakage from Jurassic sources into broadly continuous Tertiary sandstones where subsequent lateral migration occurs (Isaksen and Ledje, 2001). Vertical and lateral seals are provided by marine mudstones (Pegrum and Spencer, 1990), but complex stratigraphic alternations may occur as evidenced by the Balder Field (Hanslien, 1987; Jenssen et al., 1993). Structural and stratigraphic traps are common (Ahmadi et al., 2003), sometimes enhanced by differential compaction (Jenssen et al., 1993).

The majority of the oil resources in the study area (after data in Ministry of Petroleum and Energy, 2005) derive from the Paleogene play with 266×10^6 S m^3 (1.7×10^9 barrels) of oil recoverable and 273×10^9 S m^3 (9.6 Tcf) gas (Fig. 2). The Early and Middle Jurassic play yields large amounts of gas (157×10^9 S m^3 or 5.5 Tcf) and condensate (35×10^6 S m^3), however only insignificant oil resources (29×10^6 S m^3 or 182×10^6 barrels) (Fig. 2). The Triassic and Upper Jurassic play are of minor economic importance in the area.

In addition to the aforementioned proven plays in the area, minor oil shows have also been reported from conglomerates of Rotliegend age in Well 25/10-2R, the hydrothermally altered basement in Well 16/1-4 and in the Upper Cretaceous strata of Well 25/2-13.

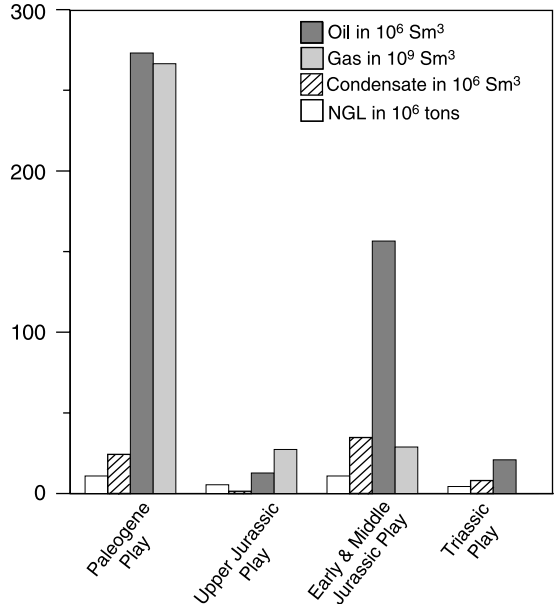

Fig. 2. Recoverable resources in the proven plays in the South Viking Graben. The resources include fields and discoveries under development or likely to be developed. Data from Ministry of Petroleum and Energy (2005).

3. Samples and analytical methods

3.1. Samples

Analyses were made on 61 oil and condensate samples provided by the Norwegian Petroleum Directorate (Table 1). In addition to these samples, published geochemical service reports for five oil samples (wells 24/12-3S, 25/11-18, 16/1-4, 25/8-9 and 25/2-12) in the area were obtained from the same source. One hundred and eighty-one source rock cutting samples of eight wells penetrating the Upper Jurassic were collected at the core repository of the Norwegian Petroleum Directorate. To complete the source rock data set, carbon isotopic data for saturate and aromatic fractions of source rock extracts were provided by Esso Norway, based on analyses performed at Geolab Nor, Robertson Research International, Simon Petroleum Technology, Geochem and the Norsk Hydro Research Center.

3.2. Analytical methods

Oil densities were determined using an Anton Paar Densimeter DMA 602 at standard conditions of 15 °C and atmospheric pressure and converted to API gravities. Solvent extraction was carried out with a SOXTEC^{TM} System HT2 1045 extraction unit on washed, crushed and ground cutting samples with dichloromethane/methanol (93:7) as solvent. In the following, asphaltenes of all samples were precipitated by adding an excess amount of *n*-pentane following the procedure suggested in Weiss et al. (2000). For GC, GCMS and isotope analysis, preparative group type separation of the maltene fraction was carried out using medium pressure liquid chromatography (MPLC) following methods modified from Radke et al. (1980). For all oil samples and the source rock extracts from wells 15/9-18, 25/5-5, 25/7-2, 16/7-2 and 25/1-10 a Merck-Hitachi 655A-12 pump and L-500 LC Controller was used together with a Shimadzu RID-10A Refractive Index Detector. Samples from wells 15/3-3, 15/3-5 and 16/1-2 were separated using a similar system with Beckman Model 100A and 112 pumps and a Gilson 131 RI Detector. A Merck Lobar Lichroprep Si 60 40–63 μm column and *n*-hexane as mobile phase was used in both cases.

An Iatroscan TH-10 TLC-FID Analyser MKII was used to determine the compound class composition of the deasphaltened oil samples.

The carbon isotopic analysis of the saturate and aromatic hydrocarbon fractions of all oil samples and 15 source rock samples of Well 15/9-18 was carried out on a Carlo Erba NA 1500 elementary analyser and a Finnigan MAT Delta E online mass spectrometer. All results are reported against the international standard PDB. GC and GC–MS analysis for the saturate fractions of all oil samples and source rock samples of wells 15/9-18, 25/5-5, 25/7-2, 16/7-2 and 25/1-10 was performed on a Hewlett Packard GCMSD,

Table 1
Sample details for analysed oils and condensates, including their assigned families. In addition to these samples, data for wells 16/1-4, 24/12-3S, 25/2-12, 25/8-9 and 25/11-18 were available from reports

Sample ID	Well	Test	Depth m TVDss	Reservoir age	Field/discovery	Family	Sample ID	Well	Test	Depth m TVDss	Reservoir age	Field/discovery	Family
1	15/5-5	T1	2128-2158	Paleocene	Glitne	A	32	16/7-4	DST1	2565-2572	Triassic	Sigyn	F
2	15/6-2	DST7	3574	Middle Jurassic	Dagny	B	33	16/7-7ST2	DST1	2538-2562	Triassic	Sigyn	F
3	15/6-3	T2	3467-3473	Middle Jurassic	Sleipner Vest	B	34	24/6-2	T1	2133-2142	Paleocene	Alvheim	C1
4	15/8-1	T3	3663-3672	Middle Jurassic	Alpha	D	35	24/9-3	DST1	1770-1779	Eocene	24/9-3	C1
5	15/8-1	T4	3618-3628	Middle Jurassic	Alpha	D	36	24/9-3	DST2	1738-1756	Eocene	24/9-3	C1
6	15/9-1	T1	3610-3635	Middle Jurassic	Sleipner Vest	C1	37	25/2-10S	RFT5	1964	Eocene	25/2-10S	C2
7	15/9-5	T2	3563-3568	Middle Jurassic	Sleipner Vest	D	38	25/2-13	DST2B	2684-2691	Cretaceous	Lille Frøy	G
8	15/9-7	T3	3530-3540	Middle Jurassic	Sleipner Vest	D	39	25/2-13	DST5	3321-3360	Middle Jurassic	Lille Frøy	G
9	15/9-8	T1	3425-3435	Middle Jurassic	Sleipner Vest	D	40	25/4-6S	DST1	3750-3767	Middle Jurassic	Vale	G
10	15/9-9	T2	2361-2367	Paleocene	Sleipner Øst	E	41	25/5-1	DST3B	2962-2977	Middle Jurassic	Frøy	G
11	15/9-9	T3	2298-2308	Paleocene	Sleipner Øst	E	42	25/5-2	DST2	3174-3179	Middle Jurassic	Frøy	G
12	15/9-A-10	T1	2272-2341	Paleocene	Sleipner Øst	E	43	25/5-3	DST1	2364-2383	Middle Jurassic	Skirne	G
13	15/9-11	T1	2772-2782	Middle Jurassic	Sleipner Øst	B	44	25/5-5	DST1	2133-2145	Paleocene	25/5-5	A
14	15/9-11	T2	2385-2407	Paleocene	Sleipner Øst	E	45	25/6-1	DST1	2251-2254	Middle Jurassic	25/6-1	G
15	15/9-11	T3	2370-2390	Paleocene	Sleipner Øst	E	46	25/7-2	DST1	4123-4248	Upper Jurassic	25/7-2	B
16	15/9-12	T1B	3560-3570	Middle Jurassic	Sleipner Vest	D	47	25/7-3	DST1	2073-2084	Paleocene	Jotun	C2
17	15/9-12	T2	3487-3497	Middle Jurassic	Sleipner Vest	D	48	25/7-5	DST1	2021-2030	Paleocene	25/7-5	C2
18	15/9-13	T1	2740-2744	Middle Jurassic	Sleipner Øst	B	49	25/8-1	T1	1746-1753	Paleocene	Ringhorne	C2
19	15/9-13	T2	2397-2402	Paleocene	Sleipner Øst	E	50	25/8-11	DST1	1875-1892	Early Jurassic	Ringhorne	C2
20	15/9-15	T1	2855-2865	Middle Jurassic	Gungne	E	51	25/8-11	T?	1875-1892	Early Jurassic	Ringhorne	C2
21	15/9-15	T2	2805-2825	Middle Jurassic	Gungne	E	52	25/8-5S	DST1	2054-2080	Paleocene	Jotun	C2
22	15/9-17	T1	2781-2791	Triassic	Loke	E	53	25/10-5	DST1	1731-1738	Eocene	Balder	C1
23	15/9-17	T2	2704-2719	Middle Jurassic	Loke	E	54	25/10-5	DST2	1707-1715	Eocene	Balder	C1
24	15/9-19A	T1A	3070-3074	Middle Jurassic	Volve	A	55	25/10-8	DST1	2367-2373	Upper Jurassic	Hanz	C2
25	15/9-19A	T2B	3017-3052	Middle Jurassic	Volve	A	56	25/11-5	DST1	1726-1741	Paleocene	Balder	C1
26	15/9-19SR	T1	2864-2880	Middle Jurassic	Volve	A	57	25/11-6	DST1	1700-1715	Paleocene	Balder	C1
27	15/12-5	T2	2913-2913	Early Jurassic	Varg	C1	58	25/11-8	DST1	1695-1710	Paleocene	Balder	C1
28	15/12-6	T1	2883-2891	Early Jurassic	Varg	C1	59	25/11-14S	T1	1786-1803	Paleocene	Balder	C1
29	15/12-6S	T2	2837-2856	Early Jurassic	Varg	C1	60	25/11-15	DST1	1712-1751	Paleocene	Grane	C1
30	15/12-8	T1	2815-2846	Triassic	15/12-8	B	61	25/11-21A	DST	1766	Paleocene	Grane	C1
31	15/12-9S	DST2	2726	Upper Jurassic	Varg	C1							

consisting of a HP 6890 GC Plus and a HP 5973 Mass Selective Detector operating in SIM mode. The GC unit was equipped with two HP 19091Z-105 HP-1 methyl siloxane columns of 50 m nominal length, 200 μm nominal diameter and 0.33 μm nominal film thickness each. The oven's initial temperature was 50 °C and increased regularly during 20 min to an end temperature of 310 °C until 80 min. Helium was used as carrier gas. The temperature of the FID was 320 °C and the hydrogen flow was 40 ml/min, while the air flow was held at 400 ml/min.

Samples of the wells 15/3-3, 15/3-5 and 16/1-2 were analysed on the same system, but using two HP 19091Z1J-102 HP-5 5% phenyl methyl siloxane columns of 25 m nominal length. The oven's initial temperature was 70 °C, increased during 20 min to an end temperature of 310 °C until 60 min and the air flow was held at 450 ml/min. GC and GCMS ratios were calculated from measured peak heights.

4. Results and discussion

4.1. Source rock geochemistry

Although several source-prone horizons have been identified in the area (Field, 1985; Thomas et al., 1985), it is generally agreed that the Oxfordian to Ryazanian Draupne Formation is the principal hydrocarbon source rock (Barnard and Cooper, 1981; Cornford, 1998; Justwan and Dahl, 2005; Justwan et al., 2005). Oil and gas is also generated by the underlying Upper Jurassic Heather Formation of Callovian to Oxfordian age. The coaly shales and coals of the Middle Jurassic Hugin and Sleipner formations (Bathonian to Oxfordian) in the southern half of the study area have potential to generate gas and minor amounts of liquid hydrocarbons (Isaksen et al., 1998). The shales of the Early Jurassic Dunlin Group are generally lean and inertinitic in the study area (Thomas et al., 1985). Therefore, for the study of genetic relations between oils and source rocks in the area, only samples from Middle and Upper Jurassic strata were used.

4.1.1. Source potential

Earlier studies (Justwan and Dahl, 2005; Justwan et al., 2005) have shown that the source facies and potential of the Jurassic source rocks in the area varies greatly regionally and stratigraphically. Within the Draupne Formation there are large differences in source potential and geochemical characteristics between the upper, post-rift section of Mid Volgian to Ryazanian age ('upper Draupne Formation') and the lower syn-rift section of Oxfordian to Mid Volgian age ('lower Draupne Formation') (Justwan and Dahl, 2005; Justwan et al., 2005). The upper Draupne, which is up to 330 m thick in the area, is generally rich oil-prone and dominated by Type II kerogen, while the up to 1600 m thick lower Draupne Formation contains a mixture of oil-prone Type II and gas-prone Type III material, with a dominance of gas-prone matter (Fig. 3) (Justwan et al., 2005). The oil-prone nature of the upper Draupne Formation is the result of widespread anoxic conditions, as well as little dilution by clastic or terrestrial organic matter (Justwan et al., 2005). The facies and potential of the lower Draupne Formation is due to dilution of the marine material with gas-prone and inert organic matter through mass flow processes and a higher degree of clastic dilution (Justwan et al., 2005). The Heather Formation is a lean, mostly gas-prone source with only few isolated patches of marine Type II kerogen source rock (Justwan et al., 2005). Maturity-corrected Hydrogen

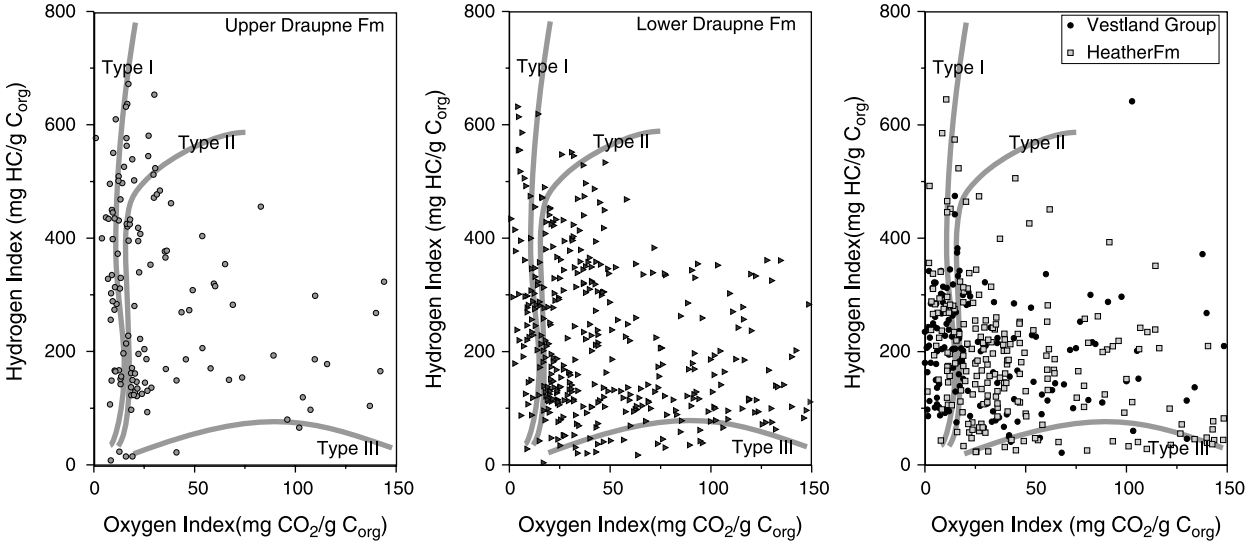

Fig. 3. Pseudo-Van Krevelen diagrams for Upper and Middle Jurassic source horizons. While the upper Draupne Formation predominantly consists of oil-prone Type II kerogen, the lower Draupne Formation is characterised by a mixture of Type III and Type II material. The Heather Formation and the Middle Jurassic Vestland Group show an even higher contribution of Type III kerogen.

Indices (HI), as well as total amount of organic carbon (TOC) values, increase gradually upwards (Fig. 4). Average values after Justwan et al. (2005) for the respective formations are: Heather Formation: Hydrogen Index of 184 g HC/kg C_{org} and 3.6 wt% TOC ($n=334$); Lower Draupne Formation: Hydrogen Index of 234 g HC/kg C_{org} and 4.1 wt% TOC ($n=520$); Upper Draupne Formation: Hydrogen Index of 340 g HC/kg C_{org} and 5.3 wt% TOC ($n=210$). The Hugin and Sleipner formations contain organic rich shales with lower TOC and HI values than the Heather Formation. In addition, they contain carbargillites and coals with TOC values well above 60 wt% (Fig. 4).

4.1.2. Molecular and isotopic characteristics of Upper and Middle Jurassic source rocks

Regional and stratigraphic variations in source potential are also reflected in molecular and isotopic properties. It is desirable to obtain profound knowledge of the molecular facies distribution within the source horizons for a source–oil correlation project. In order to extract useful information

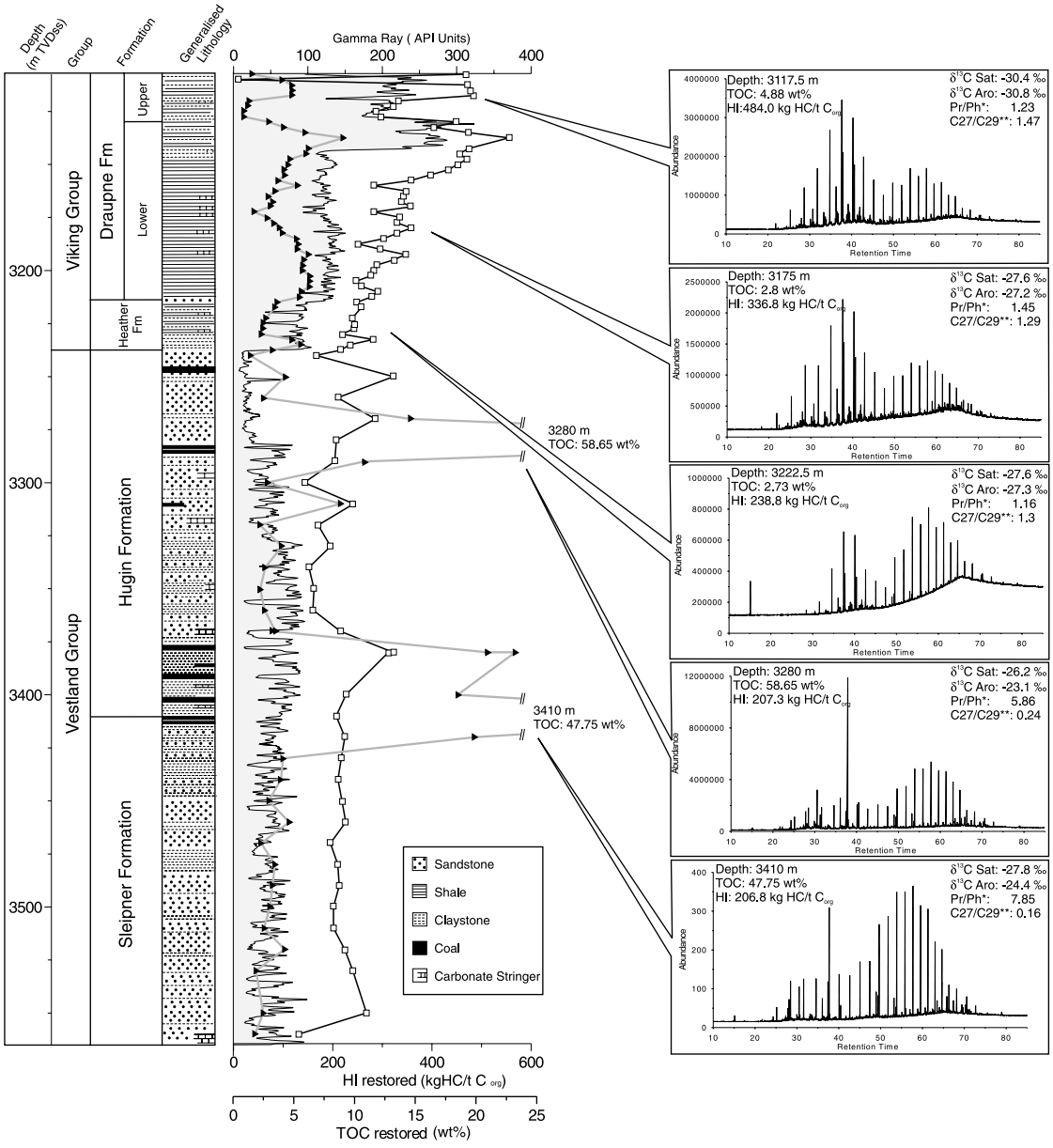

Fig. 4. Well log response, lithology, maturity-corrected TOC (triangles) and Hydrogen Index (squares) and exemplary gas chromatograms for source extracts for the Upper and Middle Jurassic section of Well 15/9-18 (well position see Fig. 1). The Draupne Formation of Oxfordian to Ryazanian age is the principal hydrocarbon source rock in the area, while the Callovian to Oxfordian Heather Formation generates gas and to minor extent oil. The Middle Jurassic Hugin and Sleipner formations (Bathonian to Oxfordian) have potential to generate gas and minor amount of liquid hydrocarbons (Isaksen et al., 2002). The Draupne Formation can be subdivided into a rich, oil-prone, upper, post-rift section of Mid Volgian to Ryazanian age and an underlying syn-rift section which contains a mixture of gas- and oil-prone kerogen (Justwan and Dahl, 2005; Justwan et al., 2005). * Ratio of Pristane over Phytane ** Ratio of C_{27} to C_{29} regular steranes, measured in *m/z* 218.

on source facies and depositional environments from biomarker data and to identify useful source–oil correlation parameters, only samples of the same level of thermal maturation and sufficient richness should be employed. However, as the kitchen areas are often only sparsely drilled even in mature exploration areas, this is difficult. Filtering the available data set to remove lean and immature samples would dramatically reduce the amount of available data; we have therefore chosen to keep the entire database. The source rock database contains samples from 2209 to 4798 m TVDss, of which more than 85% originate from depths greater than 3000 m TVDss equalling maturities of $\geq 0.5\%$ R_o according to a regional depth–vitrinite reflectance correlation. Not all geochemical parameters used in this study are affected to the same degree by thermal maturation. While the distribution of C_{27} to C_{29} ββ(R+S) regular steranes and the Pr/Ph ratio are reported to be relatively unaffected by maturation (Waples and Machihara, 1990; Peters and Moldowan, 1993; Hughes et al., 1995; Justwan et al., 2005), the ratio of C_{34} to C_{35} homohopanes, relative abundance of 17α(*H*),21β(*H*)-28,30-bisnorhopane, as well as the ratio of dia- versus regular steranes and the carbon isotopic composition can be affected by thermal maturity (Waples and Machihara, 1990; Peters and Moldowan, 1991; Peters and Moldowan, 1993; Dahl, 2004) and have to be used with care. We also used the ratio of 17β(*H*),21α(*H*)-moretane to 17α(*H*),21β(*H*)-hopane as an indicator for terrestrial input (Isaksen and Bohacs, 1995). Although moretanes are less thermally stable than 17α(*H*) hopanes and decrease in abundance with increasing maturity (Waples and Machihara, 1990), most of the transformation has been completed up to maturity levels equalling 0.6% R_o (Waples and Machihara, 1990; Peters and Moldowan, 1993).

Although *n*-alkane distributions and the Carbon Preference Index, or CPI (Bray and Evans, 1961), can be used as indicators for source facies, they are also highly dependent on maturity. We will employ these parameters only in a supportive manner.

The extracts of the Draupne Formation characteristically show low Pr/Ph ratios, with an average value of 1.38, dominance of *n*-C_{16} to *n*-C_{19} alkanes and low CPI values (Fig. 4). The terpane distribution of Draupne Formation extracts is characterised by low ratios of C_{34} to C_{35} homohopanes (averages 1.03), low relative amounts of 17β(*H*),21α(*H*)-moretane to 17α(*H*),21β(*H*)-hopane and a strong dominance of 17α(*H*),21β(*H*)-hopane over 17α(*H*),21β(*H*)-norhopane (Fig. 5). Although not present in every sample, 17α(*H*),21β(*H*)-28,30-bisnorhopane, here measured as a ratio relative to C_{30} hopane, is very common in the Draupne Formation, while it is nearly absent in the underlying Heather Formation (Fig. 5). The sterane mass fragmentograms (*m*/*z* 217 and 218) are characterised by dominance of the C_{27} ββ(R+S) regular steranes over their C_{29} homologues and a predominance of diasteranes over regular steranes. The saturate and aromatic fraction of the Draupne Formation extracts are generally isotopically lighter, with average values of −29.5‰ (δ^{13}C Sat) and −29.0‰ (δ^{13}C Aro).

Even though the exact significance of the Pr/Ph ratio is still debated (e.g. ten Haven et al., 1987), it is widely used as an indicator for the redox potential of the depositional environment (Didyk et al., 1978; Hughes et al., 1995). Commonly, values below 1 are interpreted as indicators of anoxic conditions during deposition, while values above 3 are typical for oxic environments (Didyk et al., 1978; Hughes et al., 1995). In agreement with Frimmel et al. (2004) we have used the relative changes of the Pr/Ph ratio as an indicator of changes in O_2 availability at the time of deposition. The low Pr/Ph ratios in the Draupne Formation extracts indicate deposition under anoxic to dysoxic conditions. This observation is supported by low ratios of C_{34} over C_{35} homohopanes, also associated with reducing conditions (Peters and Moldowan, 1991) and the occurrence of bisnorhopane. 17α(*H*),21β(*H*)-28,30-bisnorhopane is often called a marker for Upper Jurassic sourced oils in the North Sea (Grantham et al., 1980; Huc et al., 1985; Dahl, 2004) and although its exact origin is still under debate, it appears to be associated with anoxic environments of deposition (Katz and Elrod, 1983; Curiale and Odermatt, 1989). The Draupne Formation appears to be dominated by marine algal organic matter, as reflected by dominance of C_{27} regular steranes over the C_{29} homologues (Huang and Meinschein, 1979) and the strong dominance of C_{30} hopane over C_{30} moretane (Isaksen and Bohacs, 1995). This is also supported by the dominance of *n*-C_{15} to *n*-C_{19} alkanes, typically associated with algal input (Gelpi et al., 1970).

The molecular and isotopic compositions of the syn- and post-rift sections of the Draupne Formation are very similar. Certain properties however may allow us to differentiate between the syn- and post-rift facies, among those the Pr/Ph ratio, carbon isotopic composition and the content of 17α(*H*),21β(*H*)-28,30-bisnorhopane. The upper, post-rift facies typically shows the lowest Pr/Ph ratios, lowest C_{34}/C_{35} homohopane ratios, as well as lowest C_{30} moretane/hopane ratios (Fig. 5) and has the isotopically lightest extracts. Although there is some variation (Fig. 5), the upper Draupne Formation shows the highest relative amount of bisnorhopane. Enrichment in bisnorhopane in the Volgian to Ryazanian section appears to be a widespread feature, as it has also been observed by Kubala et al. (2003) in the neighbouring East Shetland Basin and Ineson et al. (2003) in the Danish Central Graben. The lower Draupne Formation not only exhibits slightly higher values of the Pr/Ph, C_{34}/C_{35} homohopane ratio, and the C_{30} moretane/hopane ratio and has a heavier isotopic composition, but the larger variation of geochemical parameters also suggests it has a less uniform facies (Fig. 5).

The samples of the Upper Jurassic Heather Formation have average values of −27.8‰ (δ^{13}C Sat) and −26.5‰ (δ^{13}C Aro), which is isotopically slightly lighter than

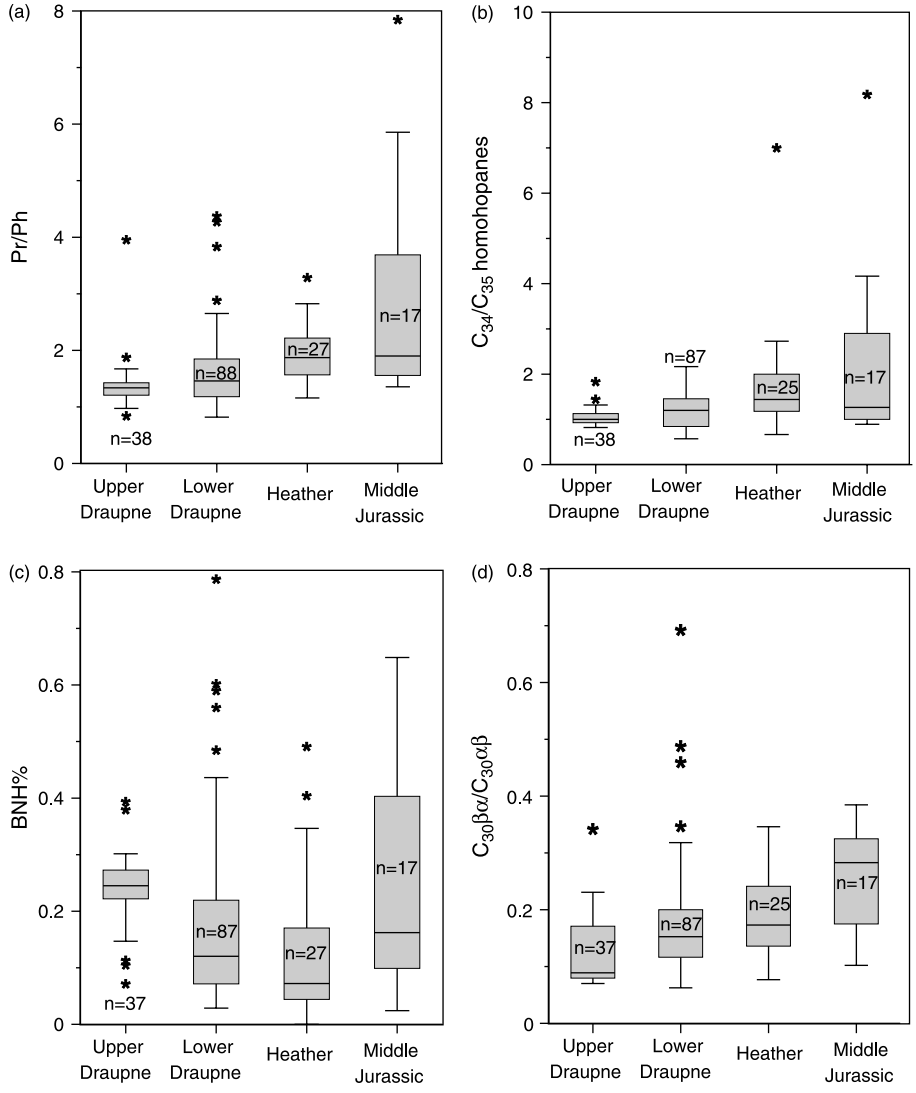

Fig. 5. Box-and-whisker plots for selected geochemical parameters for Upper and Middle Jurassic source rocks: (a) Pristane/Phytane ratio. (b) Ratio of C_{34} to C_{35} homohopanes. (c) BNH%: 17α(*H*),21β(*H*)-28,30-bisnorhopane versus 17α(*H*),21β(*H*)-28,30-bisnorhopane +17α(*H*),21β(*H*)-hopane. (d) Ratio of 17β(*H*),21α(*H*)-moretane over 17α(*H*),21β(*H*)-hopane. Second and third quartiles are displayed by the box, while the median value is indicated by the line across the box. Outliers shown as *, represent values 1.5 times the interquartile range below or above the central 50% of the distribution.

samples of Middle Jurassic age and slightly heavier than Draupne samples. Pr/Ph ratios vary between 1.16 and 3.29. The average Pr/Ph ratio for the Middle Jurassic (1.98) is however higher than the average for the Draupne Formation, indicating higher oxygen levels during deposition (Fig. 5). This is supported by the dominance of C_{34} homohopanes over the C_{35} homologues. The distribution of C_{27} to C_{29} regular steranes is distinctively different from the Middle Jurassic source, but very similar to the distribution in the Draupne Formation samples, indicating a significant marine input to the source rock. Elevated values of the ratio of C_{30} moretane to C_{30} hopane up to 0.38, suggest however higher terrestrial input in the Heather Formation than in the Draupne Formation (Fig. 5). Although 17α(*H*),21β(*H*)-28,30-bisnorhopane occurs in some samples of the Heather Formation, it is generally present in low amounts. A bimodal *n*-alkane distribution with maxima from *n*-C_{14} to *n*-C_{18} and *n*-C_{21} to *n*-C_{29} and an odd-over-even carbon number predominance in the Heather Formation samples can be interpreted as a sign of mixed input of terrestrial and marine material.

The large variability in depositional environment of the Middle Jurassic Hugin and Sleipner formations causes a great deal of variation in molecular and isotopic characteristics. Middle Jurassic source rock extracts are generally isotopically heaviest, with average values of −27.8‰ (δ^{13}C Sat) and −25.9‰ (δ^{13}C Aro). Carbargillites and coals exhibit the heaviest carbon isotopic composition. Characteristic for Middle Jurassic samples are elevated Pr/Ph ratios and C_{34}/C_{35} homohopane ratios, both indicating highly oxidizing depositional environments (Fig. 5). Carbargillites and coals again show the highest values. Pr/Ph ratios above

3 have been found characteristic for coaly shales and coals (Hughes et al., 1995).

High relative abundances of C_{29} regular steranes, as well as C_{30} moretane, and a dominance of *n*-alkanes in the range of C_{23} to C_{30} (Figs. 4 and 5) reflect dominating terrestrial input. Extreme values are associated with coals and carbargillites. 17α(*H*),21β(*H*)-28,30-Bisnorhopane is also encountered in Middle Jurassic samples. In fact the highest relative amounts of bisnorhopane of the analysed sample set occurs in the Middle Jurassic coal samples (Fig. 5). Bisnorhopane has been encountered earlier in coal samples (e.g. Mastalerz et al., 1997). This suggests that elevated relative amounts of bisnorhopane are not necessarily associated with anoxic environments and that the occurrence of bisnorhopane should not be used as the sole indicator for anoxia.

4.2. Oil and condensate properties

4.2.1. Variation of API gravity with depth

Viscosity, sulfur content, acid content, and especially oil density strongly affect the commercial value of an oil accumulation. The sample set covers a very wide range of oil densities, here expressed as API gravities, from the heavy degraded oils in 24/9-3 with 17.1° API to the very light hydrocarbons in 15/9-13 with 64.7° API (Fig. 6). This change with depth is a result of progressive cracking of carbon chains, as well as of different genetic types and secondary alteration processes. Except for 15/9-1 at 24.4° API, all samples with API gravities lower than 27° API derive from shallower depths than 2000 m TVDss. While the depth–density relation is poor for the entire data set, the correlation is greatly improved by treating Tertiary and Pre-Tertiary reservoired hydrocarbons separately. The hydrocarbons in Tertiary reservoirs show a strong depth dependency of oil density ($R^2 = 0.82$), with a rapid increase in API gravity with depth of 6.1° API/100 m (Fig. 6). A similar depth relationship was found by Barnard and Bastow (1991) in the South Viking Graben, including data from neighbouring English blocks. The hydrocarbons in Pre-Tertiary reservoirs form two groups. The first group consists only of very light hydrocarbons of above 50° API in the Greater Sleipner Area, 16/1-4, 25/6-1 and Skirne. The remaining samples show a less distinct depth–density relation, with an API increase of ca. 3° API/100 m (Fig. 6). The heaviest oil is 24.4°API in Well 15/9-1, while the lightest hydrocarbons in 25/7-2 show a gravity of 49.1°. The data show that liquid hydrocarbons with API gravities below 40° are encountered at depths down to 3635 m in the area.

4.2.2. Thermal maturity

The state of thermal maturity of the analysed oils was evaluated based on analysis of the saturate biomarkers. For this purpose, the ratios of 20S/(20S + 20R) for ααα C_{29} steranes and ββ/(αα + ββ) for 5α-C_{29} steranes have been

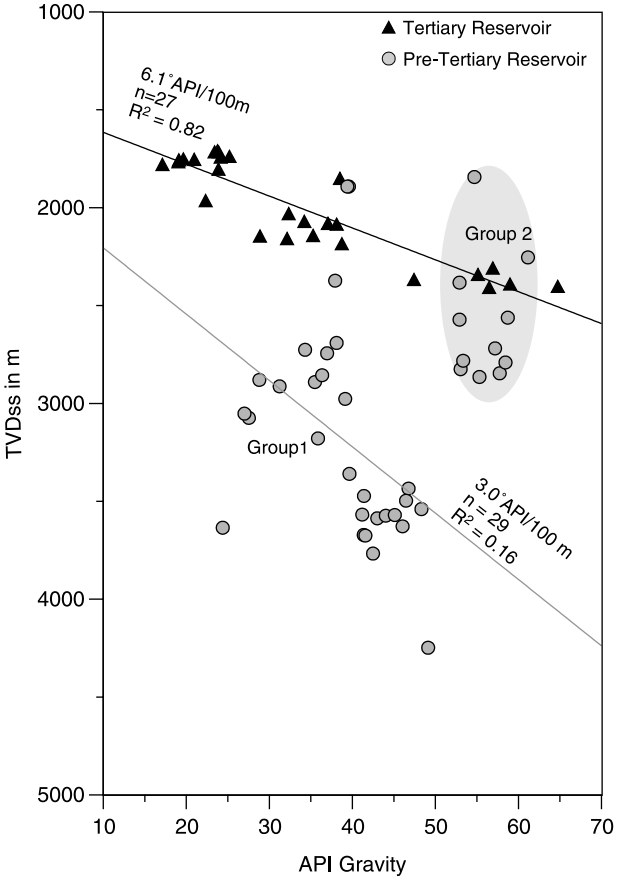

Fig. 6. Regional variation of API gravity with depth. The Tertiary reservoired hydrocarbons offer a good correlation with a rapid increase of API gravity with depth. The hydrocarbons in Pre-Tertiary reservoirs split in two groups: a group with a slower increase of API gravity of 3°/100 m (Group 1) and a high API gravity group (Group 2).

evaluated (Fig. 7) together with the ratios of 22S/(22S + 22R) for C_{32} homohopanes.

This comparison offers only a very crude way of comparison as all oils represent mixtures of fractions generated at different temperatures and times from one or more source rock units (Wilhelms and Larter, 2004). Classical biomarker parameters, such as the ones used, can show several orders of magnitude variation in concentration in end-member oils of different maturity (Wilhelms and Larter, 2004). Therefore, the maturity signature of mixed oils can be misleading (Wilhelms and Larter, 2004).

Although all samples have reached equilibrium of the C_{32} 22S/(22S + 22R) homohopane ratio, the majority of the oils in the study area have not reached equilibrium for the sterane isomerisation. This confines the maturity of the bulk of the samples to a level from onset of generation (0.6% R_o) to the early stages of main oil generation (0.8–0.9% R_o) (Peters and Moldowan, 1993). Oils from the Greater Balder Area (Grane, Jotun, Ringhorne, Balder) show 20S/(20S + 20R) sterane isomerisation ratios between 0.48 and 0.51 and 0.6–0.65 for the ββ/(αα + ββ) sterane

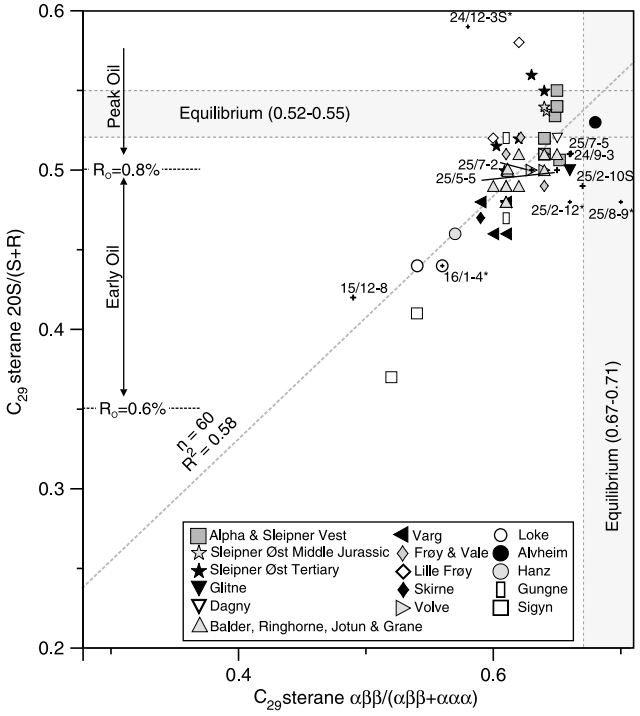

Fig. 7. Thermal maturity of the analysed oil and condensate samples based on sterane isomerisation. Vitrinite reflectance estimates after correlations in Waples and Machihara (1990); Peters and Moldowan (1993). * Data from geochemical service reports. Regression line based on own samples only.

ratio (Fig. 7). According to correlations in Waples and Machihara (1990); Peters and Moldowan (1993), this equals the beginning of peak oil generation (0.8–0.9% R_o). The samples from Volve, Gungne, Frøy, Vale, 25/7-2, 25/5-5 and 25/2-10S show similar maturities, while samples from Hanz, Skirne and Varg appear to be generated at slightly lower maturities, equalling the late phases of early oil generation (Fig. 7). The samples from Dagny, Glitne, Alvheim, 25/7-5 and 24/9-3 are slightly more mature than the Greater Balder oils. The highest maturity in the analysed data set is shown by light oils and condensates from Sleipner Vest, Øst and Alpha (15/8-1) as well as Lille Frøy (Fig. 7).

The hydrocarbons from Sigyn, Loke and 15/12-8, as well as the sample from Well 16/1-4, are outliers in the data set and show the lowest maturity. Although the C_{32} 22S/(22S + 22R) homohopane ratio has reached endpoint values (0.56–0.61), indicating maturity higher than 0.6% R_o, the sterane isomerisation ratios are low with 0.37–0.44 for the 20S ratio and 0.56–0.61 for the ββ/(αα + ββ) ratio. The values for the sterane isomerisation indicate levels of maturity equal to 0.6–0.8% R_o. This is considerably lower than the maturity of the hydrocarbons in the neighbouring Sleipner Øst and Vest fields. The maturity of the sample from Well 25/6-1 could not be evaluated properly due to low concentration of biomarkers in the sample.

4.2.3. Biodegradation

Biodegraded crude oils of varying degrees of alteration were encountered only in Tertiary reservoirs from seven fields, including the Balder, Grane, Ringhorne and Alvheim Fields as well as the 24/9-3, 25/2-10S and 25/7-5 discoveries (Table 2). The degree of biodegradation was assessed using API gravities, gross chemical composition, visual inspection of GC data and GC–MS data of the saturate hydrocarbon fractions, and the samples were ranked using the scale of Peters and Moldowan (1993).

The samples from Well 24/9-3 are most affected by biodegradation and were ranked 6 (heavy biodegradation) on the scale of Peters and Moldowan (1993). This is

Table 2
List of all biodegraded samples in order of increasing biodegradation (25/11-6 least degraded; 24/9-3 most degraded) including sample depths and corresponding reservoir temperatures

Well	Test	Depth TVDss in m	Formation	Field	Temperature (°C)	Rank[a]
25/11-6	DST1	1700-1715	Heimdal	Balder	67[b]	1+(6–7)
25/11-8	DST1	1695-1710	Heimdal	Balder	67[b]	1+(6–7)
25/11-14S	T1	1786-1803	Heimdal	Balder	70[c]	1+(6–7)
25/10-5	DST2	1707-1715	Balder	Balder	68[b]	1+(6–7)
25/11-5	DST1	1726-1741	Heimdal	Balder	68[b]	1+(6–7)
25/10-5	DST1	1731-1738	Balder	Balder	68[b]	1+(6–7)
25/8-1	T1	1746-1753	Heimdal	Ringhorne	68[b]	1+(6–7)
25/11-21A	DST	1766	Heimdal	Grane	68[c]	1+(6–7)
25/11-15	DST1	1712–1751	Heimdal	Grane	68[c]	1+(6–7)
25/11-18[d]	T2	1733	Heimdal	Grane	68[c]	1+(6–7)
25/7-5	DST1	2021–2030	Hermod	25/7-5	63[e]	4
24/6-2	T1	2133–2142	Heimdal	Alvheim	64[e]	4
25/2-10S	RFT5	1964	Frigg	25/2-10S	63[b]	6
24/9-3	DST2	1738–1756	Frigg	24/9-3	57[b]	6
24/9-3	DST1	1770–1779	Frigg	24/9-3	58[b]	6

[a] Biodegradation ranking after Peters and Moldowan (1993).
[b] Corrected log temperatures.
[c] Estimate based on field wide temperature gradient.
[d] Geochemical data obtained from Norwegian Petroleum Directorate.
[e] DST temperature.

evidenced by complete removal of the *n*-alkanes, low API gravities of 17.1 and 19.1°, respectively, and the magnitude of the unresolved complex mixture (UCM) in the C_{15+} fraction of the saturate hydrocarbons (Fig. 8), which increases with increasing degree of alteration. Further evidence for severe biodegradation is seen from the presence of 17α(*H*),21β(*H*)-25-norhopane, which is reported to derive from bacterial degradation of regular hopanes first occurring at levels of heavy biodegradation after removal of *n*-alkanes and acyclic isoprenoids (Connan, 1984; Peters and Moldowan, 1993).

Similar levels of alteration can be seen in the sample from Well 25/2-10S. It is however slightly less degraded than the samples from Well 24/9-3, judging from incomplete removal of *n*-alkanes and acyclic isoprenoids (Fig. 8) and a lower ratio of 25-norhopane to C_{30} hopane (Fig. 9). The oils from Alvheim (24/6-2) and the 25/7-5 discovery have a moderate degree of alteration, equalling rank 4 on the scale of Peters and Moldowan (1993). This is indicated by a less pronounced UCM hump and the incomplete removal of *n*-alkanes (Fig. 8). Acyclic isoprenoids appear to be only slightly affected and 25-norhopane is absent (Fig. 8).

Within this group of samples, the degree of biodegradation also covaries with the changes in compound class composition and API gravities. The relative amounts of saturated hydrocarbons decrease from 76.1 to 36.6%, while the relative amounts of aromatic hydrocarbons and NSO compounds increase with increasing degree of biodegradation. API gravities increase from 35.3% in Well 25/7-5 at rank 4 to 17.1° in Well 24/9-3 at rank 6.

The samples deriving from the Greater Utsira High Area, including the Grane, Balder and Ringhorne Fields exhibit special characteristics in terms of biodegradation. The presence of an unresolved complex mixture (Fig. 8) and ratios of 25-norhopane to C_{30} hopane between 0.19 and 0.26 (Fig. 9) indicate a severe level of biodegradation, while the gas chromatograms of the saturate hydrocarbon fraction suggest only slight alteration. The acyclic isoprenoids appear to be intact, while the short-chained *n*-alkanes underwent early stages of degradation. This is shown by comparison of a sample from Well 25/8-11 deriving from the Jurassic reservoir at Ringhorne with the Tertiary reservoired oil in 25/8-1 (Fig. 8). The oils are very similar and derive from the same source facies, they show however different abundances of short-chained alkanes. The 25/8-11 samples can be regarded as unaltered equivalents of the 25/8-1 sample.

The oils in the Tertiary reservoirs of these fields appear to be the result of at least two phases of oil charge. The initial oil charge to these oil fields was probably severely biodegraded (level 6 or 7), as evidenced by the presence of 25-norhopane. The fields were later charged with fresh oil, diluting the heavy degraded oil, and have recently undergone mild biodegradation.

The oils in the Greater Balder Area can be ranked further according to their physical and molecular properties. The Grane oils are most altered, having the largest UCM 'hump', followed by the oil from 25/8-1, whilst the least biodegraded oils of this group are in the Balder field and have the smallest UCM hump (Fig. 8). The gross geochemical composition of the Greater Balder oils cannot be directly compared to the remaining biodegraded oils due to their mixed nature. Within the Greater Balder oils however, the degree of biodegradation also covaries with API gravities and the relative amount of saturated and aromatic hydrocarbons (Fig. 8).

As mentioned earlier, only oils from Tertiary reservoirs are biodegraded, while the generally deeper and warmer Pre-Tertiary reservoirs studied are all sterile. However, the oils of the Tertiary Jotun field, for example, are evidence that not all Tertiary reservoirs are biodegraded. To assess the risk of encountering biodegraded hydrocarbons in an exploration well in the South Viking Graben, the geochemical data was related to reservoir depths and temperatures. Temperatures were taken from DST reports and wireline log readings, corrected for the effects of drilling fluid circulation. To reduce the uncertainty associated with predicting these temperatures, they have been validated by checking against regional trends and geothermal gradients from own data and the literature (e.g. Kubala et al., 2003).

The occurrence of biodegradation is strongly related to the temperature history of the reservoir and thus indirectly to reservoir depth. Bacterial life responsible for biodegradation is believed to thrive only at temperatures below 80 °C, hence this temperature is thought to represent a limit for biodegradation (Connan, 1984). The concept of sterility of reservoirs above 80 °C was refined by Wilhelms et al. (2001) suggesting pasteurization of reservoirs by deep burial in inverted basins. In the study area, which is a subsiding basin, the reservoirs are probably currently at maximum reservoir temperature.

Reservoir temperature constitutes a reliable indicator of biodegradation in the South Viking Graben, as all samples deriving from reservoirs at temperatures at or below 70 °C are biodegraded (Fig. 10). The oil rim of the Frigg field shows also biodegradation-equalling levels of 6 and is currently at reservoir temperatures of 61 °C (Larter and di Primio, 2005). In addition, no biodegradation is evident in the sample set above this temperature. Although it is generally agreed on a limit of 80 °C (Connan, 1984), regional differences might be caused by different strains of bacteria in the respective basins (Ahsan et al., 1997). Predicting biodegradation using the depth of the reservoir target is less reliable. Below a depth of 2140 m, TVDss biodegradation is absent, while 65% of the analysed samples above this depth are biodegraded (Fig. 10). The deepest occurrences of biodegradation in wells 25/2-10S, 24/6-2 and 25/7-5 are related to low reservoir temperatures

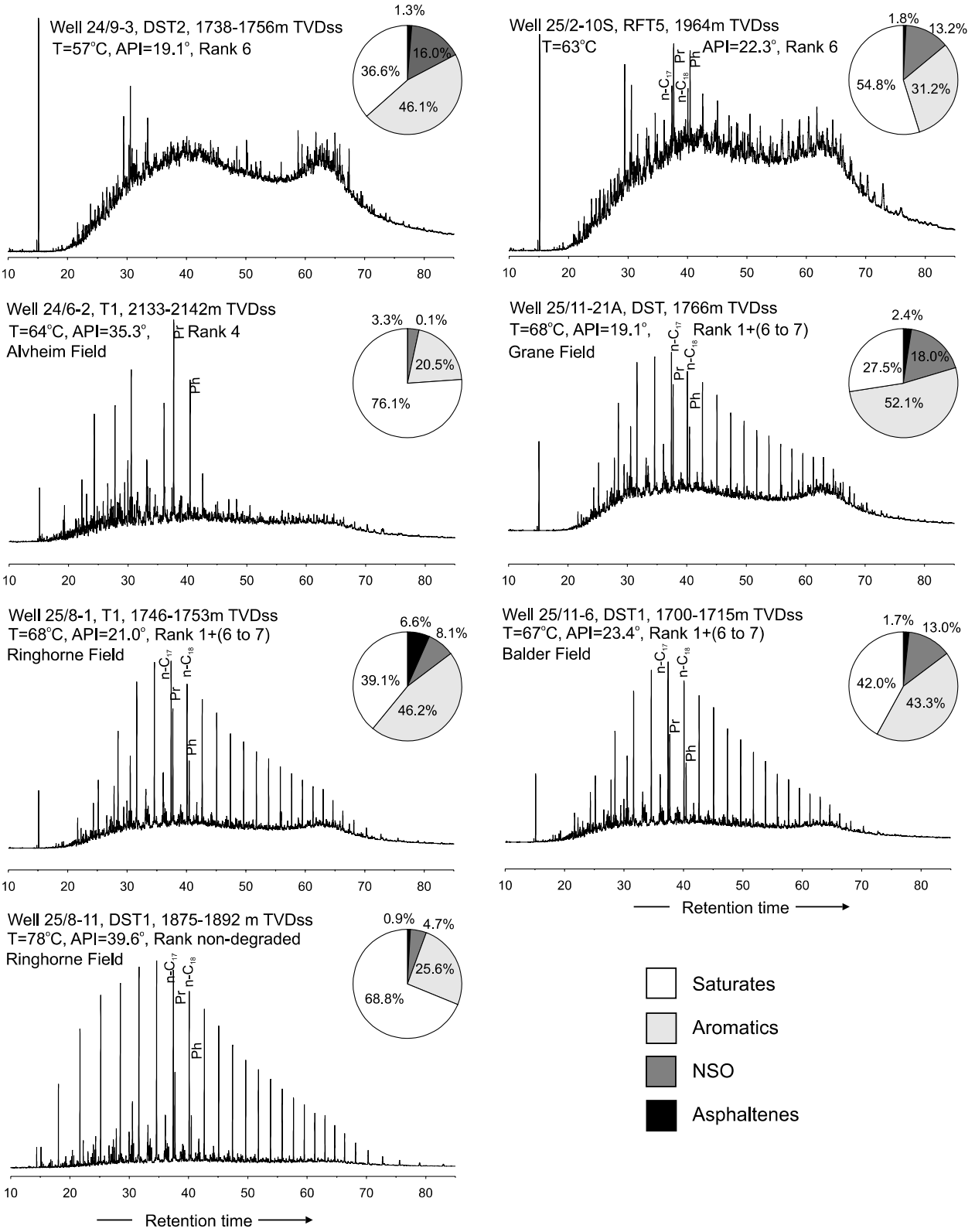

Fig. 8. Exemplary GC FID chromatograms of biodegraded samples of different levels of degradation (levels after Peters and Moldowan, 1993). Within the group of oils from wells 24/9-3, 25/2-10S and 24/6-2, the degree of biodegradation is increasing with increasing destruction of *n*-alkanes and acyclic isoprenoids, decreasing API gravities and decreasing contents of saturate hydrocarbons. The oils in wells 25/11-21A, 25/8-1 and 25/11-6 represent mixtures of a heavy degraded oil charge and a fresh charge with minor signs of alteration. The degree of degradation also increases within this group, with decreasing API gravity and contents of saturate hydrocarbons, but the samples cannot be compared to the first group due to their mixed nature. The sample from Well 25/8-11 is not degraded and has been added for comparison.

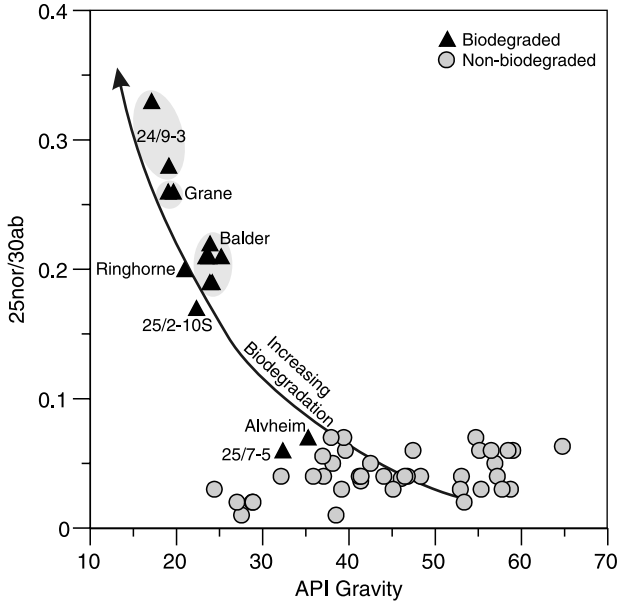

Fig. 9. Biodegradation is generally increasing with API gravity and content of 17α(*H*),21β(*H*)-25-norhopane relative to C_{30} hopane (25nor/30ab) in the sample set. The occurrence of this compound, which derives from bacterial degradation of regular hopanes, is a sign of severe biodegradation equalling levels 6 or 7 on the scale of Peters and Moldowan (1993).

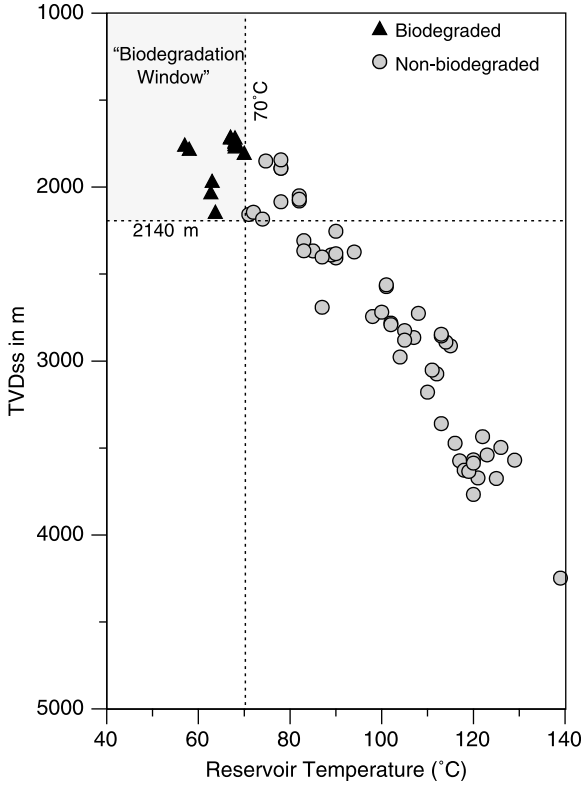

Fig. 10. Reservoir temperature-depth relationship in the South Viking Graben. Biodegraded samples are only observed in the zone above 2140 m true depth below sea-level at reservoir temperatures below 70 °C.

due to low geothermal gradients of about 3 °C/100 m, as opposed to 4 °C/100 in the Jotun area. Based on the available data the window for biodegradation in the South Viking Graben is below 70 °C and above 2140 m TVDss (Fig. 10). For more reliable predictions, filling and temperature history have to be evaluated by basin modelling.

4.3. Correlations

To establish valid oil–oil correlations, parameters have to be chosen that are not changed by maturation or secondary alteration processes. Although we have shown earlier that most of the analysed hydrocarbon samples appear to have been generated during the main phase of oil generation, we have tried to avoid using parameters for oil–oil correlation, which are too much affected by maturation. Our correlations are also based on multiple parameters in order to compensate for eventual maturity-related effects. Some samples have been affected by biodegradation, but alteration has not affected their sterane or hopane distribution. In addition to the geochemical parameters mentioned earlier we used the distribution of C_{19} to C_{25} tricyclic terpanes, which are renowned for their thermal stability (Peters, 2000) and resistance to biodegradation (Seifert and Moldowan, 1979), and are widely used in oil–oil and oil–source correlation studies (e.g. Zumberge, 1987; Chen et al., 2003). Probably most affected by maturation and secondary alteration, including migration, are the GC parameters such as Waxiness (n-C_{17}/(n-C_{17} + n-C_{27})) and Carbon Preference Index.

For oil–source correlation, ideally only source rock samples of sufficient richness and maturity should be employed. As mentioned before, we were not able to filter our source rock data set due to the limited number of samples.

4.3.1. Oil–oil correlation

By close examination of the geochemical attributes of the oils and condensates, including the above-mentioned parameters, we were able to identify seven different oil families and two subfamilies. Particularly good differentiation among hydrocarbon families is achieved with cross plots of Pr/Ph ratio and the ratio of C_{27} over C_{29} regular steranes (Fig. 11a), the ratio of C_{34}/C_{35} homohopanes (Fig. 11d), stable carbon isotope ratios (Fig. 11b) as well as the tricyclic terpane fingerprint (Fig. 12). Facies indicating biomarkers can show large variations in concentration within one petroleum system. It is therefore difficult to interpret mixed oils using classical source facies indicating biomarker ratios. In order to reliably interpret mixed oils, quantification of biomarker compounds has to be performed and used to set up a mass balance based mixing model. We have not quantified biomarker compounds in this study; hence it was not possible to set up mixing models and to determine the proportions of fractions of mixed oils. Typical examples of *m*/*z* 191 and *m*/*z* 217 fragmentograms for the oil

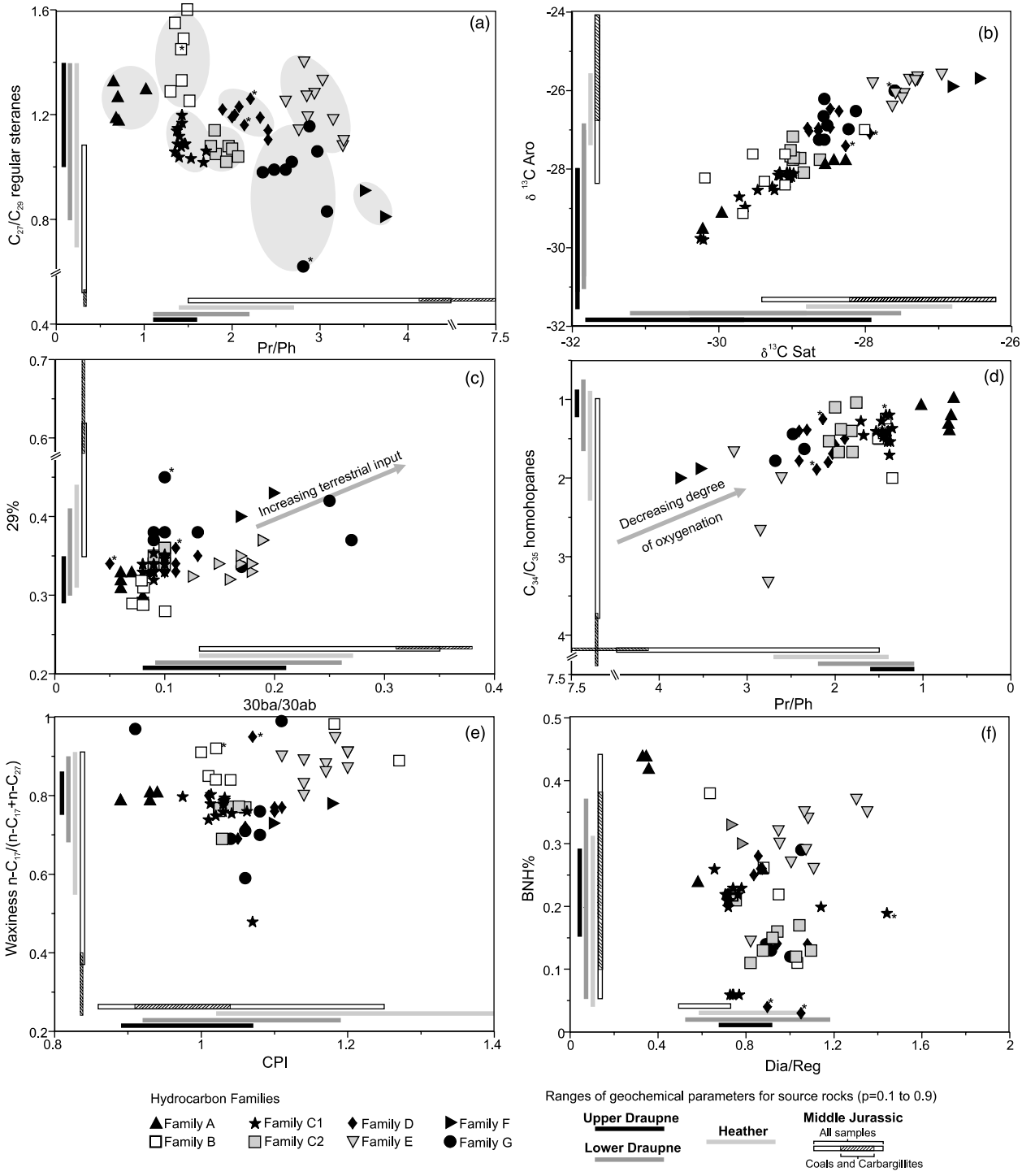

Fig. 11. Scatter plots of Pr/Ph ratio and C_{27}/C_{29} regular sterane ratio (a), carbon isotopic composition of the saturate and aromatic hydrocarbon fraction (b), abundance of C_{29} steranes relative to total abundance of C_{27}–C_{29} regular steranes and C_{30} moretane/hopane ratio (c), Pr/Ph ratio and C_{34}/C_{35} homohopane ratio (d), Waxiness and Carbon Preference Index (e), ratio of dia- versus regular steranes and relative abundance of bisnorhopane (f), for all analysed oil and condensate samples used for oil–oil correlation. Ranges for geochemical parameters for the Upper and Middle Jurassic source rock horizons ($p=0.1$–0.9) have been plotted to enable source–oil correlation (bars). To honour the different lithologies in the Middle Jurassic, ranges for shaly and coaly lithologies are plotted separately. *Data from geochemical service reports.

families are shown in Fig. 13, while biomarker ratios for the individual samples are listed in Table 3.

Family A. The uniqueness of the Volve oil within the Sleipner area and its affinity to a special, yet undrilled, Upper Jurassic source facies, has been proposed by Isaksen et al. (2002). Analysis of further samples from the South Viking Graben in this study shows that this oil type is more widespread, as oils with very similar geochemical properties

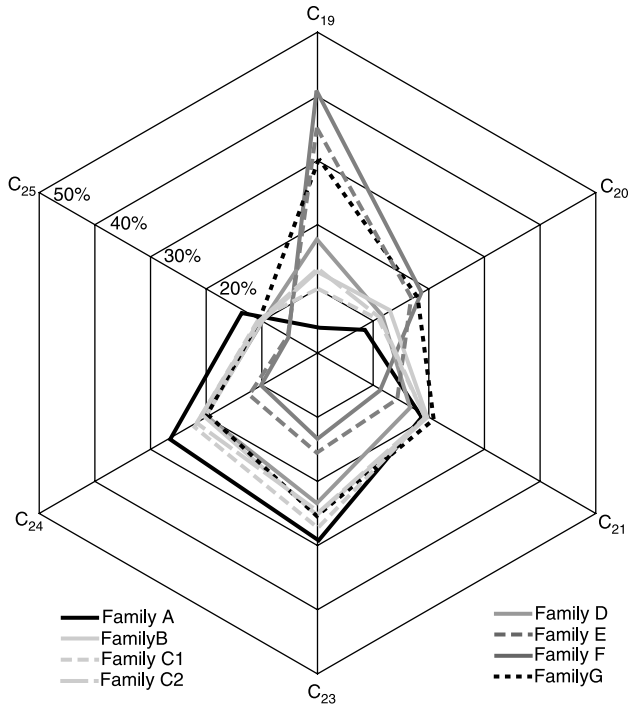

Fig. 12. Tricyclic terpane distribution for families A to G (mean values in percent for families based on normalization of the C_{19} to C_{25} tricylic terpanes).

have been found in the Well 25/5-5 and the Glitne discovery.

All samples of family A show significant amounts of 17α(*H*),21β(*H*)-28,30-bisnorhopane with special enrichment in the samples from Volve (Fig. 11f). The $\delta^{13}C$ values of the saturate fraction vary between −28.3 and −30.2‰, while the $\delta^{13}C$ values of the aromatic fraction are in the range between −27.8 and −29.5‰ (Fig. 11b). C_{27} regular steranes dominate over the C_{29} homologues, with C_{27}/C_{29} regular sterane ratios between 1.18 and 1.33. The low wax content (Fig. 11e) and the low amounts of C_{30} moretane relative to C_{30} hopane ($C_{30}\beta\alpha/C_{30}\alpha\beta$: 0.06–0.08), can be interpreted as sign of marine-dominated source facies (Gelpi et al., 1970; Huang and Meinschein, 1979; Isaksen and Bohacs, 1995). The oils have a predominance of Phytane over Pristane with Pr/Ph ratios varying from 0.7 to 1.02. The ratio of C_{34} to C_{35} homohopanes varies from 0.97 to 1.38. This can be interpreted as sign of anoxic conditions during deposition of the source rock (Didyk et al., 1978; Peters and Moldowan, 1991; Hughes et al., 1995).

The low carbon preference indices of 0.89–0.94 and the fact that regular steranes dominate over rearranged steranes (diasteranes), suggest a calcareous source facies for family A (Mello et al., 1988; Peters and Moldowan, 1993). The samples of family A share a common tricyclic terpane fingerprint, with low amounts of the C_{19} and C_{20} tricyclic terpanes and characteristic enrichment of the C_{23} and C_{24} homologues (Fig. 12).

Family B. This family includes samples from the Dagny, Sleipner Øst (Middle Jurassic) and Sleipner Vest (15/6-3) fields and the 25/7-2, 24/12-3S and 15/12-8 discoveries. Family B hydrocarbons show isotopic values of −28.0 to −30.2 ‰ for the saturate fraction and −27.6 to 29.2‰ for the aromatic fraction and a very strong dominance of the C_{27} over the C_{29} regular steranes. The abundance of C_{27} regular steranes and the pronounced dominance of C_{30} hopanes over C_{30} moretanes is here interpreted as a sign of strong marine input to the source rock (Huang and Meinschein, 1979; Isaksen and Bohacs, 1995).

Family C. This is the most widespread oil family in the South Viking Graben, including hydrocarbons in the Greater Balder Area (Balder, Grane, Ringhorne, Jotun, Hanz), the Sleipner Area (Sleipner Vest North and Varg) and Alvheim, 24/9-3, 25/7-5 and 25/2-10S. Most of the samples in family C have been affected by biodegradation. Typical features are a slight predominance of C_{27} over C_{29} regular steranes, Pr/Ph ratios below 2 (Fig. 11a) and isotopic values between −28.0 and −30.3‰ PDB for the saturate fraction and −27.6 and −29.8‰ PDB for the aromatic fraction (Fig. 11b). CPI values are commonly between 1 and 1.1. C_{30} hopane usually dominates strongly over C_{29} hopane. The tricyclic terpanes are characterised by a relative high content of C_{23} and C_{24} homologues and low contents of C_{19}. The content of C_{19} tricyclics relative to C_{23} tricylcic terpanes is however considerably higher than in family A (Fig. 12).

Based on Pr/Ph ratio, C_{27} to C_{29} regular steranes C_{34} to C_{35} homohopane distribution as well as the ratio of C_{30} moretane to C_{30} hopane, family C can be divided into two subfamilies.

The hydrocarbons in Balder, Grane, Alvheim, Sleipner Vest (15/9-1), Varg and 24/9-3 belong to subfamily C1 whose low Pr/Ph ratios of 1.37–1.7 and C_{27}/C_{29} values between 1.02 and 1.2 also indicate an anoxic to dysoxic source with marine input. The relative abundance of C_{29} regular steranes and C_{30} moretane is, however, slightly higher than in family B, indicating a less strong marine signal. The isotopic values for the saturate and aromatic fractions tend to be very similar to family B.

Subfamily C2 (including Ringhorne, Hanz, Jotun, 25/7-5, and 25/2-10S) derives from a more oxic source as shown by slightly higher Pr/Ph ratios of 1.8–2.07. The distribution of C_{27} to C_{29} regular steranes and the ratio of C_{30} moretane to C_{30} hopane are very similar to family C1. Hydrocarbons in subfamily C2 tend to be isotopically heavier than the oils in families B and C1, with values below −29.0‰ for the saturate and below −28.1‰ for the aromatic fraction. The two subfamilies have a very similar distribution pattern of tricyclic terpanes, which cannot be used to subdivide the families (Fig. 12).

Family D. Family D is distributed in the Middle Jurassic reservoirs of the southern part of the Sleipner Vest field, the Alpha discovery, as well as the Paleocene sandstones in 25/8-9 and hydrothermally altered basement in Well 16/1-4.

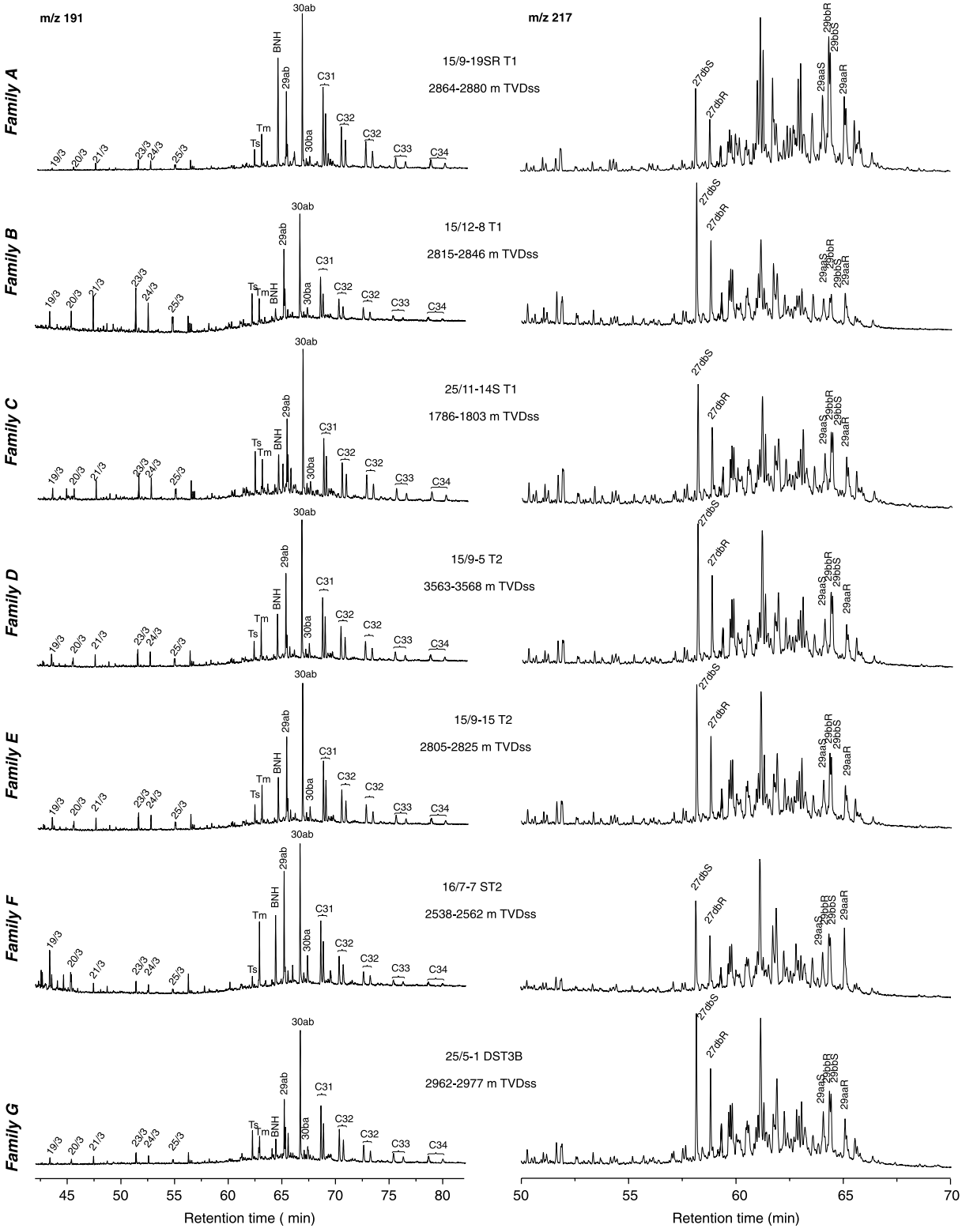

Fig. 13. Representative mass fragmentograms (*m/z* 191 and 217) for hydrocarbons of the seven main oil families in the South Viking Graben. Corresponding GC FID chromatograms see Fig. 17. Selected peaks are identified in the fragmentograms. Key: *m/z* 191: 19/3 to 25/3 = C_{19} to C_{25} tricyclic terpanes; Ts = C_{27} 18α(*H*)-22,29,30-trisnorneohopane; Tm = C_{27} 17α(*H*)-22,29,30-trisnorhopne, BNH = C_{28} 17α(*H*),21β(*H*)-28,30-bisnorhopane; 29ab = C_{29} 17α(*H*),21β(*H*)-30-norhopane; 30ab = C_{30} 17α(*H*),21β(*H*)-hopane; 30ba = C_{30} 17β(*H*),21α(*H*)-moretane; C_{31} to C_{35} = C_{31} to C_{35} 17α(*H*),21β(*H*),22(S) + (R) homohopanes. *m/z* 217: 27dbS = C_{27} 13β(*H*),17α(*H*),20(S)-cholestane; 27dbR = C_{27} 13β(*H*),17α(*H*),20(R)-cholestane; 29aaS = C_{29} 24-ethyl-5α(*H*),14α(*H*),17α(*H*),20(S)-cholestane; 29bbR = C_{29} 24-ethyl-5α(*H*),14β(*H*),17β(H),20(R)-cholestane; 29bbS = C_{29} 24-ethyl-5α(*H*),14β(*H*),17β(*H*),20(S)-cholestane; 29aaR = C_{29} 24-ethyl-5α(*H*),14α(*H*),17α(*H*),20(R)-cholestane.

Table 3
API gravities, carbon isotopic composition and saturated hydrocarbon biomarker parameters for the analysed oil and condensate samples. Parameters used in multivariate analysis are marked with *

		$\delta^{13}C$		GC parameters					Terpanes							Steranes					
ID	API	Sat	Aro	Pr/Ph*	Pr/ n-C_{17}*	Ph/ n-C_{18}*	Waxi-ness*	CPI*	19/23*	24/26*	BNH%*	30ba/ ab*	C29/ C30*	C34/ C35*	25nor/ 30ab	20S	ββ	%27*	%28*	%29*	Dia/ Reg*
1	32.1	−30.2	−29.5	1.02	0.46	0.51	0.79	0.89	0.27	1.00	0.26	0.08	0.45	1.06	0.04	0.50	0.66	0.40	0.30	0.30	0.88
2	44.0	−30.2	−28.2	1.43	0.52	0.42	0.84	1.02	0.48	1.58	0.26	0.08	0.54	1.25	0.04	0.52	0.65	0.41	0.28	0.31	0.88
3	41.4	−29.5	−27.6	1.45	0.60	0.48	0.84	1.04	0.43	1.00	0.22	0.08	0.58	1.43	0.04	0.55	0.65	0.43	0.28	0.29	0.94
4	41.4	−28.5	−26.9	2.41	0.68	0.32	0.69	1.05	0.64	1.57	0.14	0.09	0.55	1.40	0.04	0.53	0.65	0.38	0.28	0.34	0.94
5	46.1	−28.4	−26.5	2.32	0.65	0.31	0.72	1.06	0.60	1.41	0.14	0.09	0.54	1.39	0.04	0.51	0.65	0.39	0.28	0.33	1.08
6	24.4	−29.7	−28.7	1.38	0.50	0.35	0.48	1.07	0.38	2.00	0.26	0.08	0.52	1.19	0.03	0.51	0.64	0.37	0.29	0.34	0.66
7	41.2	−28.8	−27.0	2.03	0.72	0.40	0.80	1.01	0.74	1.17	0.25	0.11	0.62	1.69	0.04	0.51	0.64	0.40	0.27	0.33	0.84
8	48.3	−28.6	−27.0	2.00	0.71	0.40	0.77	1.10	0.80	1.63	0.26	0.11	0.66	1.58	0.04	0.52	0.64	0.40	0.26	0.34	0.87
9	46.8	−28.5	−26.5	2.41	0.80	0.36	0.76	1.10	1.08	2.00	0.28	0.13	0.69	1.78	0.04	0.52	0.64	0.39	0.26	0.35	0.86
10	47.4	−27.3	−25.7	3.03	0.92	0.35	0.91	1.20	2.54	2.22	0.35	0.18	1.04	n.d.	0.06	0.55	0.64	0.44	0.23	0.33	1.35
11	56.9	−27.4	−25.7	2.82	0.92	0.38	0.91	1.20	2.68	2.07	0.37	0.16	1.16	n.d.	0.05	0.56	0.63	0.45	0.22	0.32	1.30
12	55.1	−27.5	−26.1	3.15	0.93	0.33	0.89	1.14	2.24	2.30	0.26	0.15	0.78	1.67	0.06	0.52	0.62	0.40	0.26	0.34	1.11
13	53.4	−28.0	−27.0	1.35	0.72	0.62	0.91	1.00	0.42	1.26	0.38	0.07	0.58	2.00	0.02	0.54	0.64	0.45	0.27	0.29	0.64
14	56.5	−27.3	−25.7	3.26	0.93	0.32	0.90	1.11	3.23	2.75	0.34	0.19	0.93	n.d.	0.06	0.48	0.61	0.40	0.23	0.37	1.08
15	59.0	−27.3	−25.8	3.27	0.96	0.34	0.87	1.20	3.21	2.36	0.35	0.19	0.99	n.d.	0.06	0.50	0.61	0.41	0.23	0.37	1.07
16	45.1	−28.6	−27.0	2.08	0.72	0.39	0.76	1.10	0.80	2.00	0.26	0.10	0.66	1.80	0.03	0.54	0.65	0.40	0.27	0.33	0.87
17	46.5	−28.8	−27.0	1.89	0.71	0.41	0.77	1.11	0.71	1.53	0.26	0.10	0.64	1.50	0.04	0.54	0.65	0.40	0.27	0.33	0.87
18	37.0	−29.4	−28.3	1.51	0.52	0.39	0.98	1.18	0.79	1.21	0.22	0.08	0.63	1.50	0.06	0.54	0.64	0.40	0.28	0.32	0.74
19	64.7	−27.6	−26.4	2.94	0.88	0.39	0.95	1.18	1.10	3.33	0.14	0.13	0.75	n.d.	0.06	0.52	0.60	0.41	0.26	0.32	0.82
20	55.3	−27.5	−26.2	2.86	0.86	0.34	0.83	1.14	1.82	1.91	0.29	0.17	0.87	n.d.	0.03	0.52	0.61	0.41	0.25	0.34	1.07
21	53.0	−27.9	−25.8	2.76	0.87	0.34	0.80	1.14	1.61	2.11	0.27	0.17	0.78	3.33	0.04	0.47	0.61	0.40	0.25	0.35	1.01
22	58.4	−27.0	−25.6	2.85	0.94	0.37	0.88	1.17	2.56	2.53	0.30	0.18	0.88	2.67	0.06	0.44	0.54	0.43	0.23	0.34	0.95
23	57.2	−27.6	−26.1	2.61	0.90	0.38	0.86	1.17	2.31	2.27	0.32	0.18	0.88	2.00	0.04	0.44	0.56	0.43	0.23	0.34	0.95
24	27.5	−28.4	−27.8	0.70	0.59	0.97	0.81	0.93	0.14	1.75	0.44	0.06	0.48	1.38	0.01	0.51	0.64	0.41	0.27	0.32	0.35
25	27.0	−28.3	−27.8	0.68	0.60	0.98	0.79	0.93	0.14	1.50	0.44	0.06	0.48	1.19	0.02	0.50	0.63	0.39	0.28	0.33	0.33
26	28.8	−28.6	−27.9	0.71	0.55	0.86	0.79	0.89	0.13	1.75	0.42	0.07	0.49	1.30	0.02	0.50	0.64	0.39	0.27	0.33	0.36
27	31.2	−29.1	−28.3	1.37	0.53	0.43	0.76	1.03	0.36	1.17	0.06	0.09	0.50	1.53	0.03	0.46	0.61	0.38	0.29	0.33	0.74
28	35.5	−29.2	−28.5	1.40	0.51	0.41	0.75	1.02	0.32	2.30	0.06	0.09	0.46	1.53	0.03	0.46	0.60	0.38	0.29	0.33	0.73
29	36.4	−29.5	−28.5	1.38	0.46	0.38	0.74	1.01	0.33	1.50	0.06	0.10	0.53	1.70	0.03	0.48	0.59	0.38	0.29	0.33	0.74
30	57.8	−29.1	−28.4	1.49	0.61	0.51	0.89	1.27	0.39	1.03	0.11	0.10	0.68	1.50	0.03	0.42	0.49	0.45	0.27	0.28	1.03
31	34.3	−29.3	−28.4	1.43	0.50	0.40	0.78	1.03	0.27	1.17	0.06	0.09	0.53	1.44	0.03	0.48	0.61	0.39	0.29	0.32	0.77
32	52.9	−26.8	−25.9	3.52	0.95	0.29	0.78	1.18	2.70	3.50	0.30	0.17	0.78	1.88	0.03	0.41	0.54	0.36	0.24	0.40	0.78
33	58.7	−26.4	−25.7	3.75	1.04	0.30	0.73	1.10	3.44	3.75	0.33	0.20	0.81	2.00	0.03	0.37	0.52	0.34	0.23	0.43	0.74
34	35.3	−29.6	−29.0	1.43	n.d.	n.d.	n.d.	n.d.	0.48	0.63	0.20	0.08	0.46	1.45	0.07	0.53	0.68	0.38	0.29	0.33	1.14
35	17.1	−30.3	−29.8	n.d.	n.d.	n.d.	n.d.	n.d.	0.35	1.08	0.23	0.08	0.51	1.75	0.33	0.51	0.66	0.37	0.29	0.34	0.78
36	19.1	−30.2	−29.8	n.d.	n.d.	n.d.	n.d.	n.d.	0.35	1.30	0.22	0.08	0.49	1.65	0.28	0.51	0.66	0.37	0.30	0.33	0.76
37	22.3	−28.6	−27.8	n.d.	n.d.	n.d.	n.d.	n.d.	0.50	1.08	0.17	0.09	0.46	1.38	0.17	0.49	0.67	0.37	0.28	0.34	1.04
38	38.1	−28.1	−26.5	3.08	0.37	0.14	0.59	1.06	1.33	n.d.	n.d.	0.25	n.d.	n.d.	n.d.	0.52	0.60	0.35	0.23	0.42	0.97
39	39.7	−28.5	−26.9	2.61	0.47	0.22	0.69	1.04	0.50	n.d.	n.d.	0.13	0.47	n.d.	n.d.	0.58	0.62	0.38	0.24	0.38	1.01
40	42.5	−28.2	−27.0	2.68	0.49	0.21	0.76	1.08	0.85	1.50	0.12	0.09	0.46	1.78	0.05	0.49	0.64	0.38	0.25	0.37	1.00
41	39.1	−28.6	−27.3	2.35	0.61	0.30	0.70	1.08	0.67	1.90	0.14	0.10	0.46	1.63	0.03	0.51	0.61	0.37	0.25	0.38	0.89
42	35.9	−28.6	−27.3	2.48	0.57	0.27	0.71	1.06	0.70	1.67	0.13	0.09	0.48	1.44	0.04	0.52	0.62	0.38	0.24	0.38	0.91
43	52.9	−28.6	−26.2	2.88	0.60	0.27	0.97	0.91	1.98	1.24	n.d.	0.17	0.51	n.d.	n.d.	0.47	0.59	0.39	0.28	0.34	1.10

(*continued on next page*)

Table 3 (*continued*)

ID	API	$\delta^{13}C$		GC parameters					Terpanes							Steranes					
		Sat	Aro	Pr/Ph*	Pr/ *n*-C_{17}*	Ph/ *n*-C_{18}*	Waxi-ness*	CPI*	19/23*	24/26*	BNH%*	30ba/ ab*	C29/ C30*	C34/ C35*	25nor/ 30ab	20S	ββ	%27*	%28*	%29*	Dia/ Reg*
44	28.9	−30.0	−29.1	0.65	0.33	0.55	0.81	0.94	0.10	1.50	0.24	0.06	0.50	0.97	0.02	0.50	0.65	0.41	0.29	0.31	0.58
45	61.2	−28.6	−26.7	2.97	0.48	0.27	0.99	1.11	2.10	n.d.	0.29	0.27	0.65	n.d.	n.d.	0.29	0.53	0.39	0.24	0.37	1.05
46	49.1	−29.1	−27.6	1.30	0.33	0.29	0.85	1.01	0.63	n.d.	n.d.	0.00	n.d.	n.d.	n.d.	0.50	0.63	0.40	0.29	0.31	1.65
47	38.1	−29.0	−27.8	1.96	0.47	0.25	0.77	1.06	0.54	1.29	0.13	0.10	0.45	1.67	0.05	0.51	0.64	0.38	0.28	0.35	0.88
48	32.3	−29.0	−27.7	1.80	n.d.	n.d.	n.d.	n.d.	0.63	1.30	0.12	0.09	0.48	1.67	0.06	0.51	0.66	0.38	0.28	0.34	1.03
49	21.0	−28.8	−28.1	1.81	0.72	0.46	0.77	1.04	0.43	1.50	0.21	0.10	0.56	1.40	0.20	0.49	0.62	0.37	0.28	0.35	0.75
50	39.6	−28.9	−27.7	2.00	0.47	0.27	0.77	1.05	0.53	1.23	0.16	0.09	0.56	1.10	0.06	0.50	0.64	0.38	0.27	0.35	0.94
51	39.4	−29.0	−27.7	1.93	0.48	0.28	0.76	1.02	0.69	1.30	0.15	0.10	0.55	1.38	0.07	0.51	0.65	0.36	0.28	0.36	0.92
52	37.1	−29.0	−27.5	2.07	0.50	0.28	0.77	1.03	0.50	1.58	0.11	0.10	0.46	1.53	0.04	0.48	0.61	0.37	0.27	0.36	0.82
53	25.2	−29.2	−28.1	1.40	0.53	0.44	0.79	1.03	0.43	1.08	0.21	0.10	0.50	1.40	0.21	0.48	0.61	0.36	0.29	0.35	0.72
54	23.9	−29.2	−28.1	1.35	0.51	0.43	0.78	1.01	0.39	1.25	0.21	0.10	0.54	1.36	0.22	0.49	0.60	0.37	0.28	0.35	0.72
55	37.9	−29.0	−27.2	1.76	0.48	0.31	0.69	1.03	0.55	0.93	0.13	0.10	0.49	1.04	0.07	0.46	0.57	0.37	0.29	0.34	1.10
56	24.1	−29.0	−28.1	1.46	0.72	0.62	0.80	1.03	0.42	1.27	0.20	0.09	0.50	1.40	0.19	0.49	0.61	0.37	0.28	0.34	0.72
57	23.4	−29.2	−28.2	1.45	0.55	0.43	0.80	1.01	0.43	1.25	0.22	0.09	0.55	1.47	0.21	0.50	0.61	0.37	0.28	0.34	0.72
58	23.8	−29.1	−28.1	1.53	0.65	0.51	0.79	1.03	0.40	1.25	0.22	0.10	0.53	1.40	0.21	0.51	0.62	0.36	0.28	0.35	0.71
59	23.9	−29.0	−28.1	1.47	0.62	0.50	0.80	0.97	0.45	1.17	0.21	0.10	0.50	1.27	0.19	0.50	0.61	0.37	0.28	0.34	0.71
60	19.7	−29.0	−28.2	1.67	0.71	0.51	0.76	1.06	0.45	1.25	0.22	0.09	0.51	1.45	0.26	0.48	0.61	0.36	0.28	0.35	0.72
61	19.1	−29.0	−28.2	1.70	0.78	0.53	0.76	1.04	0.41	1.33	0.23	0.10	0.55	1.27	0.26	0.49	0.61	0.37	0.28	0.35	0.74

Pr/Ph: Pristane/Phytane ratio; Pr/*n*-C_{17} and Ph/*n*-C_{18}: Pristane/*n*-C_{17} and Phytane/*n*-C_{18}; Waxiness: *n*-C_{17}/(*n*-C_{17}+*n*-C_{27}); CPI: 0.5x((*n*-C_{25}+*n*-C_{27}+*n*-C_{29}+*n*-C_{31})/(*n*-C_{24}+*n*-C_{26}+*n*-C_{28}+*n*-C_{30})+(*n*-C_{25}+*n*-C_{27}+*n*-C_{29}+*n*-C_{31})/(*n*-C_{26}+*n*-C_{28}+*n*-C_{30}+*n*-C_{32})); 19/23: C_{19} tricyclic terpane/C_{23} tricyclic terpane; 24/26: C_{24} tricyclic terpane/C_{26} tricyclic terpane; BNH%: 17α(H),21β(H)-28,30-bisnorhopane/17α(*H*),21β(*H*)-28,30-bisnorhopane+17α(*H*),21β(*H*) hopane; 30ba/30ab: 17β(*H*),21α(*H*) moretane/17α(*H*),21β(*H*) hopane; C29/C30: 17α(*H*),21β(*H*)-30-norhopane/17α(*H*),21β(*H*) hopane; C_{34}/C_{35}: C_{34} 17α(*H*),21β(*H*),22(S+R) hopane/ C_{35} 17α(*H*),21β(*H*),22(S+R) hopane; 25nor/30ab: 17α(*H*),21β(*H*)-25-norhopane/17α(*H*),21β(*H*) hopane; 20S: 20S/(20S+R) ratio for C_{29}-ααα steranes; ββ: αββ/(ααα+αββ) ratios for C_{29} steranes; %27, %28, %29: relative percentages of C_{27}, C_{28} and C_{29} αββ regular steranes within C_{27} to C_{29} regular steranes, measured in *m*/*z* 218; Dia/Reg: C_{27}–C_{29} diasteranes/regular steranes; n.d.—not determined.

Family D has a generally heavier isotopic composition compared to families A, B and C and slightly higher values of Pr/Ph ratios (2.0–2.41) as well as C_{34}/C_{35} homohopane ratios (1.25–1.8) (Fig. 11d), both indicative of a higher degree of oxygenation of the source compared to families A, B and C. The C_{27} to C_{29} regular sterane ratios of 1.1–1.26 and C_{30} moretane/hopane ratios around 0.1 indicate a marine-dominated source similar to families A, B and C (Fig. 11c). Another difference from hydrocarbons in families A to C are higher ratios of C_{29} to C_{30} hopane, with an average of 0.6 compared to averages of around 0.5 in families A to C. The tricyclic terpane distribution of this group of oils is characterised by a dominance of the C_{23} and C_{24} and C_{19} homologues and low relative amounts of the C_{20} and C_{25} homologues (Fig. 12). Compared to families A to C the ratio of C_{19} to C_{23} tricyclic terpanes is considerably higher.

Family E. The hydrocarbons belonging to family E occur in the Sleipner Øst Field (Paleocene) and its Gungne and Loke satellites. The hydrocarbons have very high Pr/Ph ratios, a dominance of C_{27} over C_{29} regular steranes, a front biased *n*-alkane distribution with $n\text{-}C_{17}/(n\text{-}C_{17}+n\text{-}C_{27})$ ratios close to unity (Fig. 11f), as well as high contents of 17α(*H*),21β(*H*)-28,30-bisnorhopane. Another characteristic feature of the hydrocarbons of family E is their carbon isotopic composition. Saturate and aromatic fractions are isotopically heavier than samples belonging to families A to D, with average values of −27.4‰ for the saturate fraction and −25.9‰ for the aromatic fraction. Pr/Ph values above 2.61 and values greater than 1.67 for the C_{34}/C_{35} homohopane ratio (Fig. 11d) are indicative of a source deposited under oxidizing conditions. The distribution of C_{27} over C_{29} regular steranes suggests a marine-dominated source rock, while the high relative abundances of C_{30} moretane suggest higher terrestrial contribution. Typical for the hydrocarbons of family E is a C_{19} to C_{25} tricyclic terpane distribution dominated by the C_{19} homologues (Fig. 12).

Family F. Family F was only encountered in the Sigyn Field, located to the east of Sleipner Øst. The two samples are very light with API gravities of 52.9 and 58.7° and show very high amounts of saturated relative to aromatic hydrocarbons and NSO compounds. The samples from Sigyn are distinctively different from the rest of the data set, with the highest Pr/Ph ratios, heaviest isotopic composition of saturate and aromatic fraction, very high ratios of C_{34} to C_{35} homohopanes and high ratios of C_{30} moretane to C_{30} hopane. Pr/Ph ratios of 3.52 and 3.75 respectively, and C_{34}/C_{35} homohopane ratios of 1.88 and 2.0 indicate a highly oxygenated depositional environment, while a strong predominance of C_{29} regular steranes over C_{27} regular steranes and the high relative amounts of C_{30} moretane suggest significant terrestrial contribution to the source rock. In addition, bisnorhopane contents are very high (BNH% 0.3 and 0.33). The distribution of C_{19} to C_{25} tricyclic terpanes is very similar to the distribution in family E hydrocarbons, with dominance of the C_{19} homologue.

Family G. In contrast to how widespread families B and C are, family G is restricted to Blocks 25/2, 25/4, 25/5 and 25/6 including the Vale, Frøy, Lille Frigg and Skirne Fields as well as the Lille Frøy and 25/6-1 discoveries. Family G is the most heterogeneous group encountered in the area and the hydrocarbons of family G span a wide API gravity range between 36 and 61° (Table 3). They are isotopically heavy, with $\delta^{13}C$ values of −27.6 to −28.6 ‰ for the saturate fraction and −26 to −27.3‰ for the aromatic fraction (Fig. 11b). This renders the samples heavier than samples from families B and A and considerably lighter than hydrocarbons from family E and F. They also feature low C_{27}/C_{29} regular sterane ratios of 0.62–1.16, indicative of higher amounts of terrestrial material in the correlated source rock (Fig. 11a). The low biomarker content of the samples from Skirne, 25/2-13 DST2b and 25/6-1 complicates classification of these samples.

Especially the carbon isotopic composition suggests that 25/6-1 and Skirne are closely related to family G. The sample from Lille Frigg, Well 25/2-12, appears to be derived from an even more terrestrial source, according to the isotopic values and sterane distribution. The data were, however, obtained from geochemical service reports and the differences to the rest of family G could also be attributed to analytical variations between laboratories.

The ratios of C_{34}/C_{35} homohopanes are relatively high, which together with the high Pr/Ph ratios of 2.48 and 3.08, suggest an oxic environment of deposition for the source rock (Fig. 11d). Another distinctive feature of the family G oils and condensates are relatively low amounts of 17α(*H*),21β(*H*)-28,30-bisnorhopane and ratios of dia- versus regular steranes between 0.89 and 1.1. The tricyclic terpane fingerprint (Fig. 12) is similar to the samples of family E and F, with a strong dominance of the C_{19} homologue.

Multivariate analysis. Biomarker data for oil samples has been statistically examined by principal component analysis using the multivariate analysis tool SIRIUS® to confirm the subdivision in oil families established earlier. Principal component analysis is useful when many variables are studied simultaneously, as it reduces the dimensionality of the data by extraction of latent variables and allows description and display of complex data, possibly revealing otherwise overlooked features (Birks, 1987). This type of statistical analysis of geochemical data has proven to be a valuable tool in oil–oil correlation studies (e.g. Telnæs and Dahl, 1986; Eneogwe and Ekundayo, 2003). Relationships among the oils were determined by analysis of 15 source related biomarker parameters (Table 3). Standardisation of the data was achieved by weighting with the inverse of the standard deviation of the variables. To exclude interlaboratory variation, data originating from geochemical service reports were excluded. The samples 25/7-2, 25/5-3, 25/6-1 and 25/2-13 DST2b have also been excluded due to low concentrations of biomarkers.

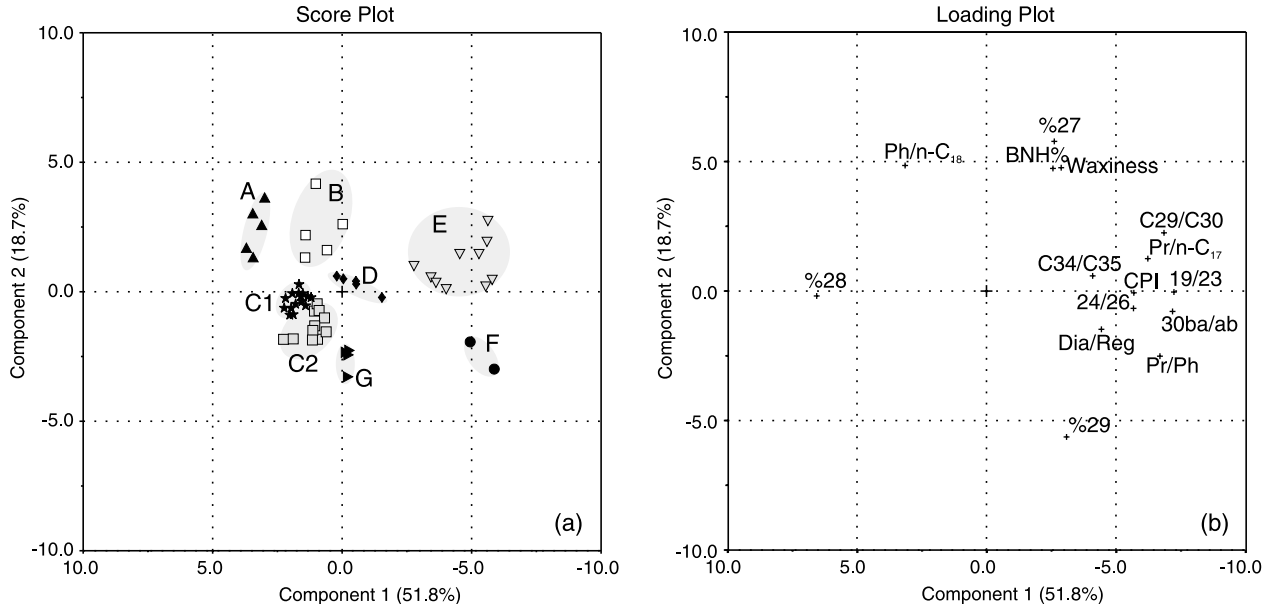

Fig. 14. Score- (a) and loading-plot (b) illustrating the results of multivariate analysis of 15 biomarker parameters of the oil and condensate dataset. Principal component 1 accounts for 51.8% of the total variance, while component 2 accounts for 18.7%. Abbreviations for parameters are explained in Table 3.

The two principal components extracted account for 70.5% of the total variance in the data set. Fig. 14 shows score- and loading plots related to the principal components. The score plot showing the relation of the analysed samples in the plane of the two principal components displays seven distinct oil families. The analysis supports the subdivision into genetic families undertaken earlier, with the exception of the samples from Well 15/8-1, which show closer affinity to family C and Well 15/9-1. Based on the values of the Pr/Ph ratio and the distribution of C_{27} to C_{29} regular steranes, we are inclined to include the samples from Well 15/8-1 in family D and the sample from Well 15/9-1 in family C1. Fig. 15 displays the result of the statistical analysis in the form of a score dendrogram, visualising dissimilarity of the samples. This display allows the identification of sub-families C1 and C2. At a high level of dissimilarity, two super-groups can be identified. Super-group 1 comprises families E and F, while super-group 2 comprises the remaining families.

4.3.2. Oil–source correlation

The seven identified oil families were genetically linked to source rocks in the area using molecular and isotopic parameters (Fig. 11). The C_{27} to C_{29} regular sterane distribution, as well as the homohopane ratio, suggests an Upper Jurassic source for family A (Fig. 11a and d). More detailed correlation is possible using stable carbon isotopes and the Pr/Ph ratio, which exclude origin from the Heather Formation (Fig. 11a and b). Family A oils are most similar to the upper Draupne facies, with high relative amounts of C_{27} regular steranes, low Pr/Ph and C_{30} moretane/hopane ratios, although Pr/Ph and C_{30} moretane/hopane ratios are lower than observed in any of the analysed source rock samples (Fig. 11). Further indication of an origin from the upper Draupne facies are the high bisnorhopane contents. We therefore conclude that the oils of family A are likely to be sourced from a highly anoxic, marine dominated, calcareous source, probably a yet undrilled facies variety of the upper Draupne Formation.

Family B is sourced from a highly algal, anoxic to dysoxic source, and the carbon isotopic composition of the saturate and aromatic hydrocarbon fractions as well as the low content of C_{30} moretane suggest an association with a Draupne source. The Pr/Ph ratio, the regular sterane distribution and the high abundance of 17α(*H*),21β(*H*)-28,30-bisnorhopane specifically indicate origin from the upper, post-rift facies. Family C1 has very similar geochemical properties to family B, although the source appears slightly less marine-dominated and is associated with the upper Draupne Formation in the same manner as Family B. Family C2 is closely related to family C1. The isotopic composition, Pr/Ph ratio and regular sterane distribution, suggest that family C2 correlates best with the shales of the lower Draupne Formation (Fig. 11). A contribution from Heather-sourced hydrocarbons cannot be ruled out.

High values of the Pr/Ph ratio and the heavier isotopic composition exclude an origin from the upper Draupne Formation shales for family D. To distinguish between an origin from the lower Draupne Formation, the Heather Formation or the Middle Jurassic is difficult. While the isotopic composition is most consistent with an origin from Middle Jurassic coals and carbargillites, the regular steranes and the C_{30} moretane/hopane ratio support a Draupne origin (Fig. 11). We argue that family D represents a mixture of hydrocarbons sourced from the Upper Jurassic Draupne

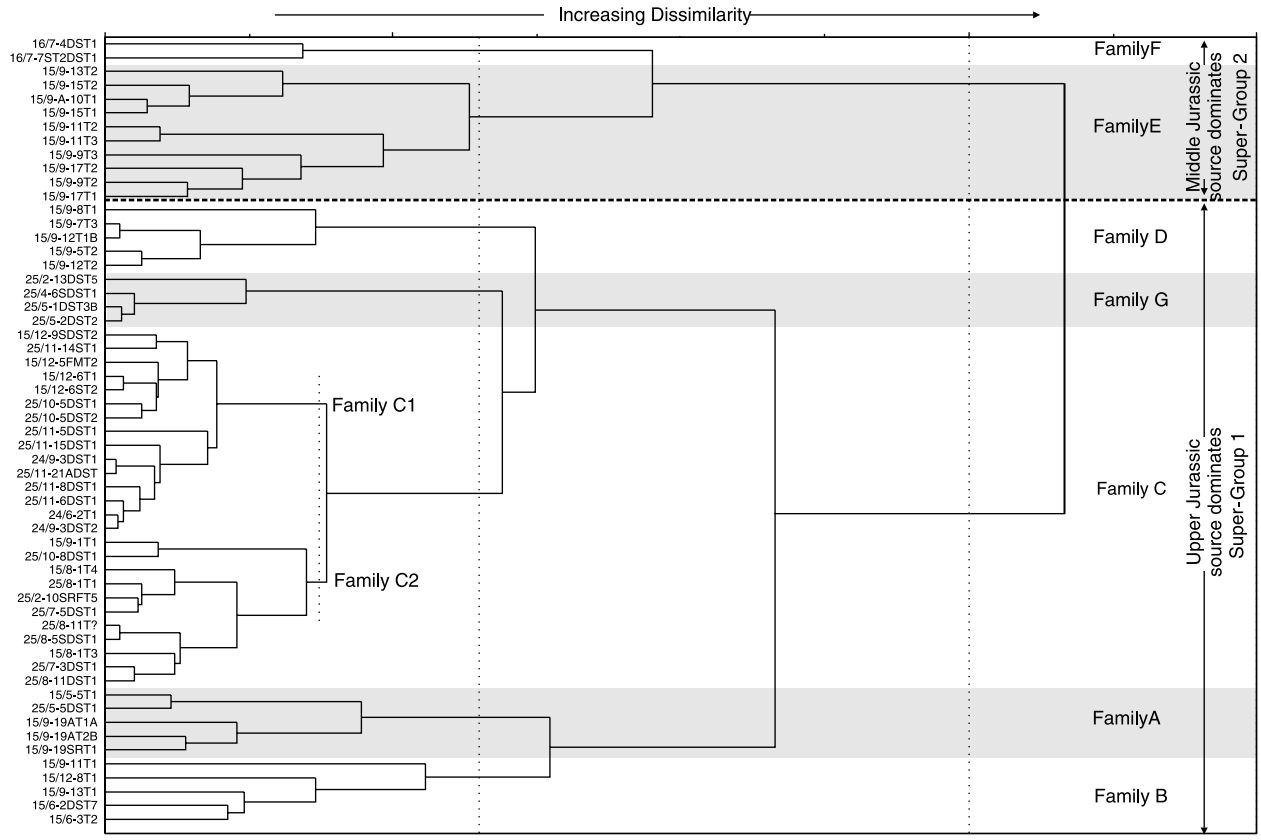

Fig. 15. Score dendrogram based on information explained by the principal components. Similar samples or clusters are joined by links, while the lengths of the branches to the links express the degree of dissimilarity. Truncation perpendicular to the branches results in clusters of samples of the same level of dissimilarity. On a high level of dissimilarity two super-groups can be identified, later linked to Upper and Middle Jurassic source rocks, while at lower levels of dissimilarity the sample set is divided into the same genetic families identified by conventional inspection of the data (apart from samples from wells 15/8-1 and 15/9-1).

Formation and the more terrestrial Heather and/or Hugin and Sleipner formations.

While elevated Pr/Ph ratios clearly associate family E hydrocarbons with a Middle Jurassic source, the regular sterane distribution measured is typically only observed in a Draupne-type source (Fig. 11). The C_{34}/C_{35} homohopane ratio and the ratio of moretane to hopane are inconclusive, while the isotopic composition clearly associates family E with coals and carbargillites of the Hugin and Sleipner formations (Fig. 11). The similarities with the Draupne Formation and Middle Jurassic extracts suggest a mixing of hydrocarbons from two sources. While the influence of the Heather Formation cannot be ruled out, family E appears to be mainly a mixture of a dominant Middle Jurassic source with a minor amount of Draupne-type hydrocarbons.

Pr/Ph ratios, stable carbon isotope ratios and the distribution of C_{34}/C_{35} homohopanes unambiguously associate family F with the Middle Jurassic Hugin and Sleipner formations. The dominance of C_{29} regular steranes and high relative amounts of C_{30} moretane are also consistent with this source. The relative amounts of bisnorhopane observed can be associated with the Draupne Formation as well as Middle Jurassic strata (Fig. 11f). Extreme values for Pr/Ph ratio and carbon isotopic composition suggest that the hydrocarbons in Sigyn represent the Middle Jurassic end-member in the study data set.

The source affinity of family G is difficult to determine. While the comparison with the regular sterane distribution and moretane abundance is inconclusive, the Pr/Ph ratio and isotopic values suggest a Heather or Middle Jurassic source, but are most consistent with a Heather source (Fig. 11).

The families can be divided into a Middle Jurassic dominated group (E and F) and an Upper Jurassic dominated group (A–D and G). These super-groups have also been identified with hierarchical cluster analysis (Fig. 15). A list of all families and their correlative source horizons is shown in Table 4.

4.4. Regional exploration implications

Based on the affiliation with the aforementioned genetic hydrocarbon families, we have analysed the contribution of the respective source families and their associated source rocks to the total assigned recoverable resources in the study area (Fig. 16). The results clearly show the overwhelming

Table 4
List of oil families and their associated correlative source rocks

Genetic family	Source depositional environment	Correlative (main) source rock horizon(s)
A	Highly anoxic, marine, calcareous	Upper Draupne Fm, undrilled facies
B	Anoxic to dysoxic, highly algal	(Upper?) Draupne Fm
C1	Anoxic to dysoxic, algal	(Upper?) Draupne Fm
C2	Dysoxic, algal	Draupne Fm
D	Mixture of anoxic to dysoxic, algal and oxic, terrestrial	Draupne + Heather/Middle Jurassic
E	Mixture of oxic, terrestrial and anoxic to dysoxic, algal	Middle Jurassic + Draupne/Heather
F	Oxic, strongly terrestrial, coaly	Middle Jurassic
G	Oxic, terrestrial	Heather Fm

dominance of Draupne sourced hydrocarbons belonging to family A, B and C. While the Draupne Formation sourced over 96% of the recoverable oil resources with 262×10^6 S m^3, the Heather Formation sources only 3% or 9×10^6 S m^3 of the oil. The remaining 52×10^6 S m^3 of recoverable oil, mainly from the Heimdal Field and the 15/3-1S, 15/3-4 and 24/9-5 discoveries, were not classified as no samples were available for familial association. All of the condensate resources accounted for are sourced by the Middle Jurassic Hugin and Sleipner Formation or represent mixtures of Upper and Middle Jurassic sources. Of the four proven play concepts, the Upper Jurassic source and Tertiary reservoir, is most prolific. Of all assigned recoverable Draupne-sourced oils 91% (239×10^6 S m^3) are reservoired in the Tertiary.

The analysis of the geographical and stratigraphical distribution of the identified oil families and their geochemical properties gives important insights into the migration patterns of the area. One important observation, based on the available dataset, is that Tertiary reservoirs contain, with exception of Well 25/8-9 and wells 15/9-11, 13 and 9 in Sleipner Øst, exclusively hydrocarbons sourced from the Upper Jurassic Draupne Formation. The Pre-Tertiary reservoirs on the other hand show a complex picture of mixing in the Sleipner Area, with three active source horizons, the Draupne and Heather Formation as well as the Middle Jurassic Vestland Group including the Hugin and Sleipner formations.

The Heather-sourced family G was only found in Pre-Tertiary reservoirs in Blocks 25/2, 4, 5 and 6 (Fig. 17). No samples from the oil rim of the Frigg gas field or the condensate of the Heimdal Field were available for analysis. Recent studies by Larter et al. (2000) and di Primio (2002) suggest that family G hydrocarbons occur in the Tertiary reservoirs of Frigg and Heimdal. The results of the present study support the conclusions of di Primio (2002) who suggested a genetic relationship between the Vale, Lille Frøy, Skirne and 25/6-1 based on analysis of PVT data. According to di Primio (2002), Vale represents the primordial fluid. After migrating through Lille Frøy, Frøy and Skirne, Well 25/6-1 contains the residual liquid phase of the migrating vapour. Also Bhullar et al. (1999) proposed a terrestrial-dominated source, most likely the Heather Formation for Lille Frøy, but proposed a different drainage area for Frøy and a distal Draupne anoxic source. The close affinity of Lille Frøy to Frøy demonstrated in this study (e.g. Fig. 15) supports a common source and a migration from Vale towards 25/6-1. Lille Frigg seems to have a separate drainage area from the rest of the group, as also indicated in Kubala et al. (2003). A detailed discussion of reservoir filling and migration in the Greater Heimdal Area is beyond the scope of this paper and is discussed in Bhullar et al. (1998, 1999), Larter et al. (2000); di Primio (2002); Ritter et al. (2000).

South of the Heather-sourced system, three Draupne-sourced accumulations have been identified in Pre-Tertiary reservoirs (Fig. 17), all probably sourced through short distance migration from nearby shales. 25/7-2 and 25/10-8 both have a Draupne sandstone reservoir, have however a different drainage area after maps in Kubala et al. (2003). The hydrocarbons in 25/8-11 are contained in the Early

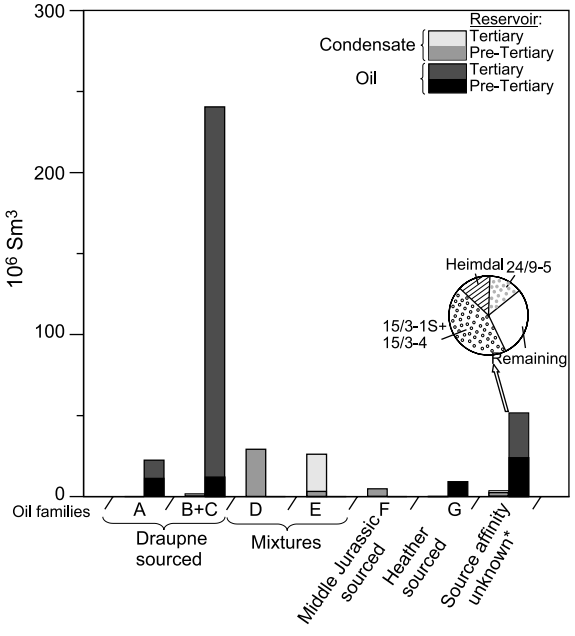

Fig. 16. Contribution of the identified hydrocarbon families to the total recoverable oil and condensate resources. For each family the split in Tertiary and Pre-Tertiary reservoirs is indicated. *Not every field or discovery was sampled during this study and its hydrocarbons linked to a source rock.

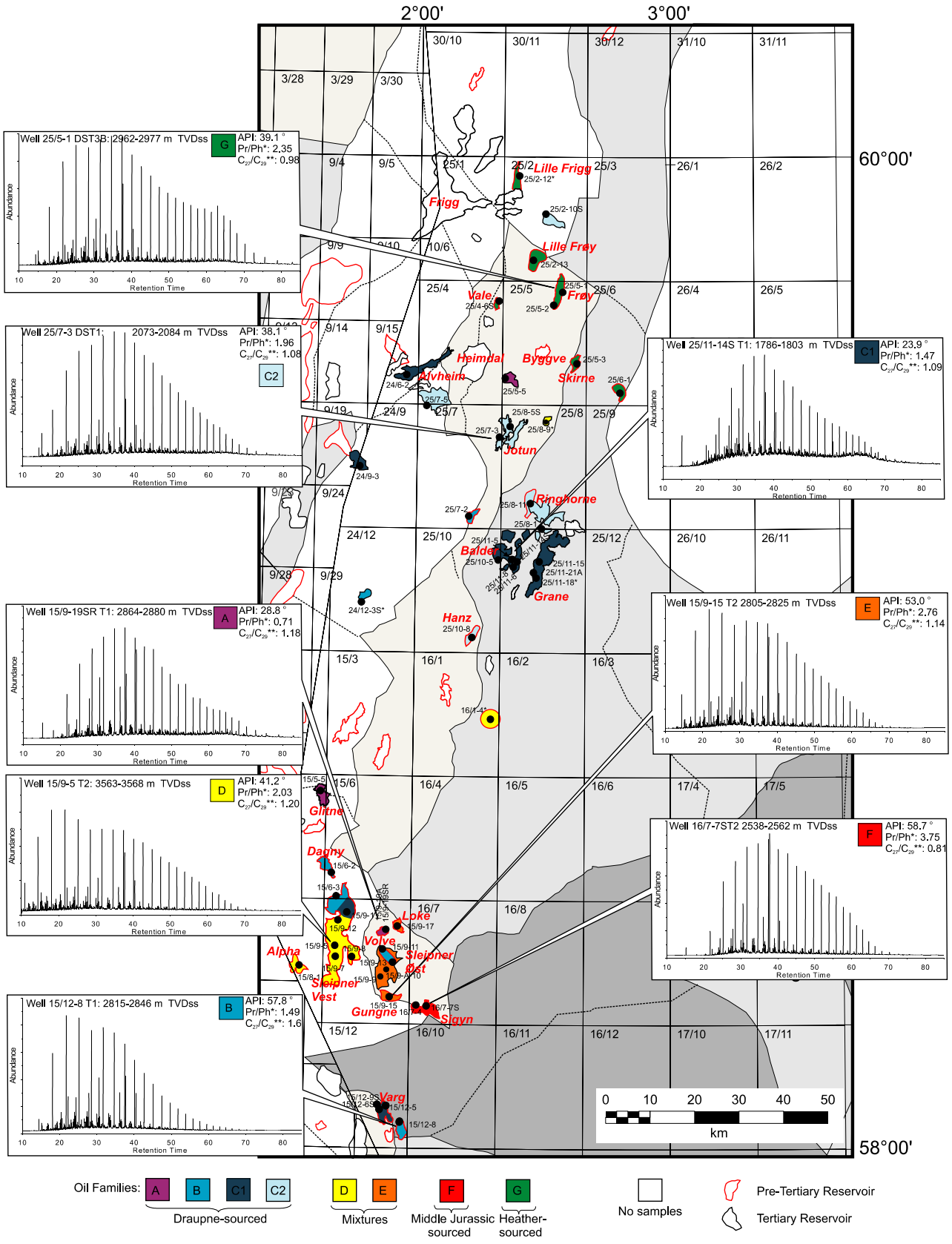

Fig. 17. Regional distribution of oil families in Tertiary (black outline) and Pre-Tertiary (red outline) reservoirs. Exemplary gas chromatograms for representative samples for each family are shown together with values for API gravity data, ratio of Pristane over Phytane (*) and ratio of C_{27} to C_{29} regular steranes (**). *m/z* 191 and 217 mass fragmentograms for respective samples of each family are shown in Fig. 13.

Jurassic Statfjord Formation and are probably sourced by lower Draupne Formation shales to the west.

The Greater Sleipner Area offers a different situation with at least two active source rock horizons leading to a variable degree of mixing between hydrocarbon charges from Middle to Upper Jurassic sources in the Pre-Tertiary reservoirs (Fig. 17). The distribution of families and their properties in the Sleipner area leads to certain constraints on migration in the area. Based on the concept that a reservoir serves as an 'integrator' of hydrocarbons of varied facies and maturities in progressively subsiding basins, we can use maturity indicators and mixing to elucidate migration in the area. The hydrocarbons categorised earlier as derived from the Upper Jurassic Draupne Formation, e.g. from wells 15/6-3 or 15/9-1, show relatively high maturities, while the Middle Jurassic end-member in Sigyn is relatively low mature. Mixing of different levels of these two sources should represent these trends in varying degree.

The northern part of Sleipner Vest is, as shown before, sourced from Draupne shales, probably to the N, E and W of Sleipner (Isaksen et al., 2002). The southern part of Sleipner Vest and Alpha represent mixtures of Upper and Middle Jurassic sources. The southern part of Sleipner Vest appears to be separated by a flow barrier from the northern part, as the distribution of oil families shows. This has been observed earlier by Isaksen et al. (2002). The hydrocarbons in Sigyn appear to be low maturity products sourced from the Middle Jurassic. Migration into Sigyn occurred probably through Gungne, which shows higher maturity possibly due to later mixing with products from Upper Jurassic source rocks. This implies that the pathway from Gungne to Sigyn has been shut off after Sigyn was filled with Middle Jurassic sourced hydrocarbons. The hydrocarbons in Loke are also comparably low mature, but show evidence of later mixing with higher maturity and more marine dominated hydrocarbons. According to Isaksen et al. (2002), Gungne and Loke fed the Tertiary reservoir of Sleipner Øst. Hydrocarbons in the Pre-Tertiary reservoirs of Sleipner Øst show affinity to Draupne Formation hydrocarbons and also higher maturity levels. To elucidate further the migration and charge history in the Sleipner area, detailed geohistory and migration modelling has to be carried out.

Also the Middle Jurassic reservoirs of Sleipner Øst are sourced from the Draupne Formation probably from a similar source area as the north of Sleipner Vest. The hydrocarbons in Volve represent an exception and are likely to be sourced from a subbasin between Sleipner Øst and Vest (Isaksen et al., 2002).

The Tertiary fields, as mentioned before, are dominated by hydrocarbons sourced from the Draupne Formation (Fig. 17). Only the hydrocarbons in Sleipner Øst however represent a mixture of hydrocarbons sourced from terrestrial and marine dominated rocks, which spilled over from the Middle Jurassic reservoirs in Loke and Gungne (Isaksen et al., 2002).

The general migration model for the Tertiary fields in the area requires a basin to margin pathway with vertical fault leakage (Isaksen and Ledje, 2001; Kubala et al., 2003). The fields on the Utsira High are fed through migration up fault planes along the western flank of the high (Barnard and Bastow, 1991; Kubala et al., 2003). Balder and Grane oils have common source and maturity characteristics and the fields also share a drainage polygon within the Tertiary system (Kubala et al., 2003), while Ringhorne to the north appears to have a slightly different source facies. The present degree of biodegradation and the occurrence of 25-norhopane in Grane, Jotun and Ringhorne, indicates a multiple charge history. The hydrocarbons in 25/8-9 are different from the nearby Jotun field. Although the sample was not analysed at the same laboratory and some differences could be attributed to analytical variation between laboratories, biomarker data suggest clearly that the source for the hydrocarbons in 25/8-9 is more oxic than the average Draupne sourced oil. The hydrocarbons are a mixture of marine and terrestrial sources with characteristics very similar to the hydrocarbons in Sleipner Vest and higher maturity than Jotun hydrocarbons. This suggests that Jotun and 25/8-9 have different migration histories: while the Jotun field is probably charged from the graben area in Block 25/7, 25/8-9 received hydrocarbons from the north, as suggested by the migration routes within the Tertiary system in Kubala et al. (2003).

5. Conclusions

Detailed geochemical characterisation of 66 oil samples from 31 fields and discoveries in the Norwegian South Viking Graben has revealed that the oil and condensate samples can be grouped in seven families and two subfamilies based on correlation using molecular and isotopic characteristics. Pr/Ph ratio, distribution of C_{27} to C_{29} regular steranes, carbon isotopic composition of the saturate and aromatic fractions and distribution of tricyclic terpanes offer the most reliable oil–oil correlation. The grouping in hydrocarbon families was supported by the results of principal component analysis of the data set using 15 selected molecular parameters.

The identified families and subfamilies have been related to three source horizons, the Upper Jurassic Draupne and Heather formations and the Middle Jurassic Vestland Group, based on correlation with geochemical parameters of 181 source rock samples. One family is purely sourced from Middle Jurassic strata (F), three families (comprising two subfamilies) derive from the Upper Jurassic Draupne Formation (A, B, C1, C2), one family appears to be sourced from the Heather Formation (G), while the remaining families (D, E) are mixtures of the aforementioned families.

The analysed samples exhibit a wide range of API gravities from 17.1 to 64.7°. Two depth trends are evident in the sample set. The samples in Tertiary reservoirs show

a strong API-depth relation with an increase of 6.1°/100 m while hydrocarbons in Pre-Tertiary reservoirs are only loosely correlated with a 3.0°/100 m increase. Liquid hydrocarbons can be encountered as deep as 3635 m.

The majority of the samples represent generation between onset (0.6% R_o) and early stages of main oil generation (0.8–0.9% R_o), as inferred from sterane and hopane isomerisation. The highest level of maturity is shown by samples from the Sleipner Øst and Vest, whereas the light oils and condensates of Sigyn and Loke show lower levels of maturity.

The geographic and stratigraphic distribution of oil families gives insight into the general migration pattern in the area. Family G, Heather-sourced, is restricted to the north of 59°30′. The Greater Sleipner area received hydrocarbons from Upper and Middle Jurassic sources leading to complex mixing. The hydrocarbons in the north of Sleipner Vest represent the end-member for the Upper Jurassic, while the light oil and condensate in Sigyn represent the Middle Jurassic end-member. The Tertiary reservoirs analysed in the area are, apart from Sleipner Øst, sourced exclusively from different source facies of the Draupne Formation.

Projections of recoverable oil volumes based on the established genetic families and their related source rocks have proven that the Upper Jurassic Draupne Formation is the major source of oil in the South Viking Graben. Eighty-four percent of the recoverable oil resources could be assigned to source rocks based on the correlations, of which 97% are sourced by the Draupne Formation alone. Of the four proven play concepts in the area, the combination of a Tertiary reservoir and Draupne Formation source, proves to be the most prolific with 239×10^6 S m^3 of recoverable oil.

Biodegradation is however common in Tertiary reservoirs. Biodegradation was not evident in Pre-Tertiary reservoirs. Based on the available data, the zone of biodegradation in the area comprises reservoirs at depths above 2140 m and present day reservoir temperatures below 70 °C. Exceptionally deep occurrences of biodegraded hydrocarbons are related to local minima of the geothermal gradient.

Acknowledgements

The authors would like to thank the Norwegian Petroleum Directorate for the release of sample material and Esso Exploration and Production Norway A/S for all the data received and permission to publish this study. Jørgen Bojesen-Koefoed and Peter Nytoft at GEUS are thanked for the use of the MPLC system and technical assistance in the laboratory. Comments on earlier versions of the manuscript by Aurélie Nowinski are greatly acknowledged. The manuscript has benefited from the constructive reviews by A.M. Spencer, B.J. Johannesen and an anonymous reviewer. This project is funded by the Research Council of Norway (Grant NFR 157825/432) and Esso Exploration and Production Norway A/S.

References

Ahmadi, Z.M., Sawyers, M., Kenyon-Roberts, S., Stanworth, C.W., Kugler, K.A., Kristensen, J., Fugelli, E.M.G., 2003. Paleocene. In: Evans, D., Graham, C., Armour, A., Bathurst, P. (Eds.), The Millennium Atlas: Petroleum Geology of the Central and Northern North Sea. Geological Society, London, pp. 235–260.

Ahsan, A., Karlsen, D.A., Patience, R.L., 1997. Petroleum biodegradation in the Tertiary reservoirs of the North Sea. Marine and Petroleum Geology 14 (1), 55–64.

Barnard, P.C., Bastow, M.A., 1991. Petroleum generation, migration, alteration, entrapment and mixing in the central and northern North Sea. In: England, W.A., Fleet, A.J. (Eds.), Petroleum Migration. Geological Society Special Publication 59, pp. 167–190.

Barnard, P.C., Cooper, B.S., 1981. Oils and source rocks of the North Sea area. In: Illing, L.V., Hobson, G.D. (Eds.), Petroleum Geology of the continental shelf of North-West Europe: Proceedings of the 2nd Conference. Heyden and Son, London, pp. 169–175.

Bhullar, A.G., Karlsen, D.A., Backer-Owe, K., Seland, R.T., Le Tran, K., 1999. Dating reservoir filling; a case history from the North Sea. Marine and Petroleum Geology 16 (7), 581–603.

Bhullar, A.G., Karlsen, D.A., Holm, K., Backer-Owe, K., Le Tran, K., 1998. Petroleum geochemistry of the Frøy Field and Rind discovery, Norwegian continental shelf; implications for reservoir characterization, compartmentalization and basin scale hydrocarbon migration patterns in the region. Organic Geochemistry 29 (1-3), 735–768.

Birks, H.J.B., 1987. Multivariate analysis in geology and geochemistry; an introduction. Chemometrics and Intelligent Laboratory Systems 2 (1-3), 15–28.

Bray, E.E., Evans, E.D., 1961. Distribution of n-paraffins as a clue to recognition of source beds. Geochimica et Cosmochimica Acta 22 (1), 2–15.

Chen, J., Liang, D., Wang, X., Zhong, N., Song, F., Deng, C., Shi, X., Jin, T., Xiang, S., 2003. Mixed oils derived from multiple source rocks in the Cainan oilfield, Junggar Basin, Northwest China; Part I, Genetic potential of source rocks, features of biomarkers and oil sources of typical crude oils. Organic Geochemistry 34 (7), 889–909.

Connan, J., 1984. Biodegradation of crude oils in reservoirs. In: Brooks, J., Welte, D.H. (Eds.), Advances in Petroleum Geochemistry. Academic Press, London, pp. 298–335.

Cornford, C., 1998. Source rocks and hydrocarbons of the North Sea. In: Glennie, K.W. (Ed.), Petroleum Geology of the North Sea; Basic Concepts and Recent Advances. Blackwell, Oxford, pp. 376–462.

Curiale, J.A., Odermatt, J.R., 1989. Short-term biomarker variability in the Monterey Formation, Santa Maria Basin. Organic Geochemistry 14 (1), 1–13.

Dahl, B., 2004. The use of bisnorhopane as a stratigraphic marker in the Oseberg Back Basin, North Viking Graben, Norwegian North Sea. Organic Geochemistry 35 (11-12), 1551–1571.

Didyk, B.M., Simoneit, B.R.T., Brassell, S.C., Eglinton, G., 1978. Organic geochemical indicators of palaeoenvironmental conditions of sedimentation. Nature 272 (5650), 216–222.

di Primio, R., 2002. Unraveling secondary migration effects through the regional evaluation of PVT data; a case study from Quadrant 25, NOCS. Organic Geochemistry 33 (6), 643–653.

Eneogwe, C., Ekundayo, O., 2003. Geochemical correlation of crude oils in the NW Niger Delta, Nigeria. Journal of Petroleum Geology 26 (1), 95–103.

Eriksen, S.H., Andersen, J.H., Grist, M., Stoker, S., Brzozowska, J., 2003. Oil and gas resources. In: Evans, D., Graham, C., Armour, A., Bathurst, P. (Eds.), The Millennium Atlas: Petroleum Geology of the Central and Northern North Sea. Geological Society, London, pp. 345–358.

Field, J.D., 1985. Organic geochemistry in exploration of the northern North Sea. In: Thomas, B.M., Doré, A.G., Larsen, R.M., Home, P.C., Eggen, S.S. (Eds.), Petroleum Geochemistry in exploration of the Norwegian Shelf. Graham and Trotman, London, pp. 39–57.

Fraser, S.I., Robinson, A.M., Johnson, H.D., Underhill, J.R., Kadolsky, D.G.A., Connell, R., Johannessen, E.P., Ravnas, R., 2003. Upper Jurassic. In: Evans, D., Graham, C., Armour, A., Bathurst, P. (Eds.), The Millennium Atlas: Petroleum Geology of the Central and Northern North Sea. Geological Society, London, pp. 289–316.

Frimmel, A., Oschmann, W., Schwarck, L., 2004. Chemostratigraphy of the Posidonia Black Shale, SW Germany I, Influence of sea-level variation on organic facies variation. Chemical Geology 206, 199–230.

Gelpi, E., Schneider, H., Mann, J., Oro, J., 1970. Hydrocarbons of geochemical significance in microscopic algae. Phytochemistry 9 (3), 603–612.

Goldsmith, P.J., Hudson, G., van Veen, P., 2003. Triassic. In: Evans, D., Graham, C., Armour, A., Bathurst, P. (Eds.), The Millennium Atlas; Petroleum Geology of the Central and Northern North Sea. Geological Society, London, pp. 105–127.

Grantham, P.J., Posthuma, J., de Groot, K., 1980. Variation and significance of the C-27 and C-28 triterpane content of a North Sea core and various North Sea crude oils. Physics and Chemistry of the Earth 12, 29–38.

Hanslien, S., 1987. Balder. In: Spencer, A.M. (Ed.), Geology of the Norwegian oil and gas fields. Graham & Trotman, Norwell, pp. 193–201.

Huang, W.Y., Meinschein, W.G., 1979. Sterols as ecological indicators. Geochimica et Cosmochimica Acta 43 (5), 739–746.

Huc, A.Y., Irwin, H., Schoell, M., 1985. Organic matter quality changes in an Upper Jurassic shale sequence from the Viking Graben. In: Thomas, B.M., Doré, A.G., Eggen, S.S., Home, P.C., Larsen, R.M. (Eds.), Petroleum Geochemistry in exploration of the Norwegian Shelf. Graham and Trotman, London, pp. 179–183.

Hughes, W.B., Holba, A.G., Dzou, L.I., 1995. The ratios of dibenzothiophene to phenanthrene and pristane to phytane as indicators of depositional environment and lithology of petroleum source rocks. Geochimica et Cosmochimica Acta 59 (17), 3581–3598.

Husmo, T., Hamar, G.P., Høiland, O., Johannessen, E.P., Rømuld, A., Spencer, A.M., Titterton, R., 2003. Lower and Middle Jurassic. In: Evans, D., Graham, C., Armour, A., Bathurst, P. (Eds.), The Millennium Atlas: Petroleum Geology of the Central and Northern North Sea. Geological Society, London, pp. 129–156.

Ineson, J.R., Bojesen-Koefoed, J.A., Dybkjaer, K., Nielsen, L.H., 2003. Volgian-Ryazanian 'hot shales' of the Bo Member (Farsund Formation) in the Danish Central Graben, North Sea; stratigraphy, facies and geochemistry. In: Ineson, J.R., Surlyk, F. (Eds.), The Jurassic of Denmark and Greenland, Geological Survey of Denmark and Greenland Bulletin 1, pp. 403–436.

Isaksen, G.H., Bohacs, K.M., 1995. Geological controls of source rock geochemistry through relative sea level; Triassic, Barents Sea. In: Katz, B.J. (Ed.), Petroleum Source Rocks. Springer, Berlin, pp. 25–50.

Isaksen, G.H., Curry, D.J., Yeakel, J.D., Jenssen, A.I., 1998. Controls on the oil and gas potential of humic coals. Organic Geochemistry 29 (1-3), 23–44.

Isaksen, G.H., Ledje, K.H.I., 2001. Source rock quality and hydrocarbon migration pathways within the greater Utsira High area, Viking Graben, Norwegian North Sea. AAPG Bulletin 85 (5), 861–883.

Isaksen, G.H., Patience, R., van Graas, G., Jenssen, A.I., 2002. Hydrocarbon system analysis in a rift basin with mixed marine and nonmarine source rocks; the South Viking Graben, North Sea. AAPG Bulletin 86 (4), 557–591.

Jenssen, A.I., Bergslien, D., Rye-Larsen, M., Lindholm, R.M., 1993. Origin of complex mound geometry of Paleocene submarine-fan sandstone reservoirs, Balder Field, Norway. In: Parker, J.R. (Ed.), Petroleum geology of Northwest Europe; Proceedings of the 4th Conference. Geological Society, London, pp. 135–143.

Johnson, H.D., Fisher, M.J., 1998. North Sea plays; geological controls on hydrocarbon distribution. In: Glennie, K.W. (Ed.), Petroleum Geology of the North Sea; Basic Concepts and Recent Advances. Blackwell, Oxford, pp. 463–547.

Justwan, H., Dahl, B., 2005. Quantitative Hydrocarbon Potential Mapping and Organofacies Study in the Greater Balder Area, Norwegian North Sea. In: Doré, A.G., Vining, B. (Eds.), Proceedings of the 6th Petroleum Geology Conference: North-West Europe and Global Perspectives. Geological Society, London, pp. 1317–1329.

Justwan, H., Dahl, B., Isaksen, G.H., Meisingset, I., 2005. Late to Middle Jurassic source facies and quality variations, South Viking Graben, North Sea. Journal of Petroleum Geology 28 (3), 241–268.

Katz, B.J., Elrod, L.W., 1983. Organic geochemistry of DSDP Site 467, offshore California, middle Miocene to lower Pliocene strata. Geochimica et Cosmochimica Acta 47 (3), 389–396.

Kubala, M., Bastow, M., Thompson, S., Scotchman, I., Øygard, K., 2003. Geothermal regime, petroleum generation and migration. In: Evans, D., Graham, C., Armour, A., Bathurst, P. (Eds.), The Millennium Atlas: petroleum geology of the central and northern North Sea. Geological Society, London, pp. 289–315.

Larter, S.R., Aplin, A.C., Bowler, B., Lloyd, R., Zwach, C., Hansen, S., Telnæs, N., Sylta, Ø., Yardley, G., Childs, C., 2000. A drain in my graben; an integrated study of the Heimdal area petroleum system. Journal of Geochemical Exploration 69-70, 619–622.

Larter, S.R., di Primio, R., 2005. Effects of biodegradation on oil and gas field PVT properties and the origin of oil rimmed gas accumulation. Organic Geochemistry 36 (2), 299–310.

Mastalerz, M., Stankiewicz, A.B., Salmon, G., Kvale, E.P., Millard, C.L., 1997. Organic geochemical study of sequences overlying coal seams; example from the Mansfield Formation (Lower Pennsylvanian), Indiana. International Journal of Coal Geology 33 (4), 275–299.

Mello, M.R., Gaglianone, P.C., Brassell, S.C., Maxwell, J.R., 1988. Geochemical and biological marker assessment of depositional environments using Brazilian offshore oils. Marine and Petroleum Geology 5 (3), 205–223.

Milton, N.J., Bertram, G.T., Vann, I.R., 1990. Early Paleogene tectonics and sedimentation in the central North Sea. In: Hardman, R.F.P., Brooks, J. (Eds.), Tectonic events responsible for Britain's Oil and Gas Reserves. Geological Society Special Publication 55, pp. 339–351.

Ministry of Petroleum and Energy, 2005. Facts 2005—The Norwegian Petroleum Activity. Norwegian Ministry of Petroleum and Energy, Oslo. 194 pp.

Pegrum, R.M., Spencer, A.M., 1990. Hydrocarbon plays in the northern North Sea. In: Brooks, J. (Ed.), Classic petroleum provinces. Geological Society Special Publication 50, pp. 441–470.

Peters, K.E., 2000. Petroleum tricyclic terpanes; predicted physicochemical behavior from molecular mechanics calculations. Organic Geochemistry 31 (6), 497–507.

Peters, K.E., Moldowan, J.M., 1991. Effects of source, thermal maturity, and biodegradation on the distribution and isomerization of homohopanes in petroleum. Organic Geochemistry 17 (1), 47–61.

Peters, K.E., Moldowan, J.M., 1993. The biomarker guide; interpreting molecular fossils in petroleum and ancient sediments. Prentice Hall, Englewood Cliffs. 363 pp.

Radke, M., Willsch, H., Welte, D.H., 1980. Preparative hydrocarbon determination by automated Medium Pressure Liquid Chromatography. Analytical Chemistry 52, 406–411.

Ranaweera, H.K.A., 1987. Sleipner Vest. In: Spencer, A.M. (Ed.), Geology of the Norwegian Oil and Gas fields. Graham & Trotman, London, pp. 253–263.

Ritter, U., Zwach, C., Sylta, Ø., 2000. Hydrocarbon leakage-fill-spill patterns in the Heimdal area, Viking Graben. Journal of Geochemical Exploration 69-70, 679–683.

Seifert, W.K., Moldowan, J.M., 1979. The effect of biodegradation on steranes and terpanes in crude oils. Geochimica et Cosmochimica Acta 43 (1), 111–126.

Stewart, I.J., 1987. A revised stratigraphic interpretation of the early Palaeogene of the central North Sea. In: Brooks, J., Glennie, K.W. (Eds.), Petroleum Geology of North West Europe, Proceedings of the 3rd Conference. Graham & Trotman, London, pp. 557–576.

Stow, D.A.V., Bishop, C.D., Mills, S.J., 1982. Sedimentology of the Brae Oilfield, North Sea; fan models and controls. Journal of Petroleum Geology 5 (2), 129–148.

Telnæs, N., Dahl, B., 1986. Oil-oil correlation using multivariate techniques. Organic Geochemistry 10 (1–3), 425–432.

ten Haven, H.L., de Leeuw, J.W., Rullkoetter, J., Sinninghe-Damste, J.S., 1987. Restricted utility of the pristane/phytane ratio as a palaeoenvironmental indicator. Nature 330 (6149), 641–643.

Thomas, B.M., Møller-Pedersen, P., Whitaker, M.F., Shaw, N.D., 1985. Organic facies and hydrocarbon distributions in the Norwegian North Sea. In: Thomas, B.M., Doré, A.G., Larsen, R.M., Home, P.C., Eggen, S.S. (Eds.), Petroleum Geochemistry in exploration of the Norwegian Shelf. Graham and Trotman, London, pp. 3–26.

Waples, D.W., Machihara, T., 1990. Application of sterane and triterpane biomarkers in petroleum exploration. Bulletin of Canadian Petroleum Geology 38 (3), 357–380.

Weiss, H.M., Wilhelms, A., Mills, N., Scotchmer, J., Hall, P.B., Lind, K., Brekke, T., 2000. NIGOGA: The Norwegian Guide to Organic Geochemical Analyses .. (accessed 22.10.2004) http://www.npd.no/engelsk/nigoga/default.htm.

Wilhelms, A., Larter, S.R., 2004. Shaken but not always stirred. Impact of petroleum charge mixing on reservoir geochemistry. In: Cubitt, J.M., England, W.A., Larter, S.R. (Eds.), Understanding Petroleum Reservoirs: towards an Integrated Reservoir Engineering and Geochemical Approach. Geological Society Special Publication 237, pp. 27–35.

Wilhelms, A., Larter, S.R., Head, I., Farrimond, P., di Primio, R., Zwach, C., 2001. Biodegradation of oil in uplifted basins prevented by deep-burial sterilization. Nature (London) 411 (6841), 1034–1037.

Ziegler, P.A., 1992. North Sea rift system. Tectonophysics 208, 55–75.

Zumberge, J.E., 1987. Prediction of source rock characteristics based on terpane biomarkers in crude oils; a multivariate statistical approach. Geochimica et Cosmochimica Acta 51 (6), 1625–1637.